Increased Temperature Disrupts the Biodiversity–Ecosystem Functioning Relationship

Elodie C. Parain,[1,2,*] Rudolf P. Rohr,[1,*] Sarah M. Gray,[1,†] and Louis-Félix Bersier[1,†,‡]

1. Department of Biology—Ecology and Evolution, University of Fribourg, Chemin du Musée 10, 1700 Fribourg, Switzerland;
2. Department of Ecology and Evolutionary Biology, Yale University, New Haven, Connecticut 06520

Submitted April 27, 2018; Accepted September 25, 2018; Electronically published December 26, 2018

Online enhancements: appendixes. *Dryad data:* https://dx.doi.org/10.5061/dryad.hk1h26n.

ABSTRACT: Gaining knowledge of how ecosystems provide essential services to humans is of primary importance, especially with the current threat of climate change. Yet little is known about how increased temperature will impact the biodiversity–ecosystem functioning (BEF) relationship. We tackled this subject theoretically and experimentally. We developed a BEF theory based on mechanistic population dynamic models, which allows the inclusion of the effect of temperature. Using experimentally established relationships between attack rate and temperature, the model predicts that temperature increase will intensify competition, and consequently the BEF relationship will flatten or even become negative. We conducted a laboratory experiment with natural microbial microcosms, and the results were in agreement with the model predictions. The experimental results also revealed that an increase in both temperature average and variation had a more intense effect than an increase in temperature average alone. Our results indicate that under climate change, high diversity may not guarantee high ecosystem functioning.

Keywords: global warming, biodiversity ecosystem functioning, Lotka-Volterra mechanistic model, competition, *Sarracenia purpurea* communities.

Introduction

Biodiversity is of critical importance for maintaining the functioning of ecosystems. With high species diversity, an ecosystem is expected to be more effective at processing nutrients and providing ecosystem services than one with low species diversity (Cardinale et al. 2002, 2006; Hooper et al. 2012; Loreau 2000, 2010). This relationship, known as the biodiversity–ecosystem functioning (BEF) relationship, has been widely demonstrated to occur in a broad range of ecosystems (Tilman et al. 1997; Hector et al. 1999; Tilman et al. 2001; Hooper et al. 2005; O'Connor et al. 2017). Maintaining high biodiversity is suggested as key for conserving ecosystem services under current global change (Perkins et al. 2015). However, little is known about how global warming will impact this relationship. Climate change models predict an increase in both average temperature and temperature variation (IPCC 2014). It is therefore important to determine whether diverse ecosystems will still maintain their functioning and ability to provide ecosystem services of high standard and, thus, whether a positive BEF relationship will still hold under an increase in temperature and temperature variability.

Among all the possible mechanisms that have been found to drive the BEF relationship, the selection effect and interspecific complementarity are considered to be the two key mechanisms (Tilman et al. 2014). The selection effect is based on the increasing probability that more diverse communities contain species with particular functional traits that allow them to be competitively superior and to drive the high productivity of a community. Interspecific complementarity posits that different species in a community have different traits, which will increase the likelihood that the community will exploit all resources and will result in higher productivity (Loreau 2010). Although their relative importance was heavily debated among ecologists, it has been recognized that these two mechanisms are not mutually exclusive (Loreau et al. 2002), with both mechanisms found to be equally important in terrestrial systems but the complementarity effect prevailing in aquatic systems (Cardinale et al. 2011).

When investigating the effect of global warming on the BEF relationship, a general statement for the selection effect is difficult to reach because of the idiosyncratic behavior of species in experiments. However, temperature is known to affect metabolism in a predictable way for a large range of ectothermic species, notably by increasing the rate at which resources are exploited (Dell et al. 2011). Consequently, a theory can be reached for the effect of warming on the BEF relationship through the mechanism of exploitative interspecific competition, which is mediated by attack rate. This pro-

* These authors contributed equally, and both served as lead authors.
† These authors contributed equally.
‡ Corresponding author; email: louis-felix.bersier@unifr.ch.
ORCIDs: Parain, http://orcid.org/0000-0001-5074-5957; Rohr, http://orcid.org/0000-0002-6440-2696; Bersier, http://orcid.org/0000-0001-9552-8032.

Am. Nat. 2019. Vol. 193, pp. 227–239.
DOI: 10.1086/701432

cess is intimately linked to niche overlap and can be seen as a counterpart of interspecific complementarity (Loreau 2010).

Here, we developed a theory based on a mechanistic consumer-resource model and compared our theoretical predictions to experimental results from a simple, natural microcosm system consisting of protozoans and bacteria (consumers and resources, respectively). This model allows the exploration of how the exploitative competition—or interspecific complementarity—is affected by temperature by using experimentally established relationships between temperature and consumer attack rates on resources. This approach enables a comprehension of how climate change can modify community dynamics through altering species interactions and demographic parameters and ultimately of how this translates in terms of the BEF relationship.

From a Consumer-Resource to a BEF Model

We based our theoretical approach on the classical Lotka-Volterra model that describes consumer-resource dynamics. For simplicity, we present here the equations for the biomass of a set of S consumers (C_i) that exploit a single resource (R); however, the model can be extended to several individual resources and to resources considered as one or several continuous niche axes (see app. A, sec. A1; table 1 provides definitions for all variables and parameters; apps. A–E are available online). We use the following Lotka-Volterra model (MacArthur 1970; Logofet 1992; Loreau 2010):

$$\begin{aligned} \frac{dC_i}{dt} &= C_i\left(-m_i - \sum_{j=1}^{S}\gamma_{ij}C_j + \varepsilon_i a_i R\right), \\ \frac{dR}{dt} &= R\left(r_R - \alpha_R R - \sum_{j=1}^{S} a_j C_j\right). \end{aligned} \tag{1}$$

The parameters of the model are as follows: $m_i > 0$, the mortality rate of consumer i; $a_i > 0$, the attack rate on the resource; $\varepsilon_i > 0$, the efficiency of transforming resource into consumers; $r_R > 0$, the growth rate of the resource; $\alpha_R > 0$, the intraspecific competition of the resource; and γ_{ij}, the interactions between consumers i and j other than exploitative competition for the common resource (e.g., interference, territorial defense, facilitation). Intraspecific competition self-limits the growth of the resource, such that in the absence

Table 1: Variables and parameters

Variable/parameter	Definition	Equation/sign constraint
R	Biomass of the resource	
r_R	Growth rate of the resource	$r_R > 0$
α_R	Intraspecific competition of the resource	$\alpha_R > 0$
K_R	Carrying capacity of the resource	$K_R = r_R/\alpha_R$
S	Number of consumers	
C_i	Biomass of consumer i	
m_i	Mortality rate of consumer i	$m_i > 0$
ε_i	Efficiency of transforming resource into consumer i	$\varepsilon_i > 0$
a_i	Attack rate on the resource by consumer i	$a_i > 0$
γ_{ij}	"Nontrophic" interaction: interactions between consumers i and j (effect of consumer j on consumer i) other than exploitative competition for the common resource R	No sign constraint on γ_{ij}; $\gamma_{ii} > 0$
r_i	Intrinsic growth rate of consumer i (the difference between m_i and the gain in fecundity from feeding on R)	$r_i = -m_i + \varepsilon_i a_i r_R/\alpha_R$
K_i	Carrying capacity of consumer i	$K_i = \dfrac{r_i}{\alpha_{ii}^{\text{eff}}} = \dfrac{-m_i + \varepsilon_i a_i r_R/\alpha_R}{\gamma_{ii} + \varepsilon_i a_i a_i/\alpha_R}$
α_{ij}^{eff}	Effective interaction: "nontrophic" interaction and exploitative competition between consumers i and j	$\alpha_{ij}^{\text{eff}} = \gamma_{ij} + \varepsilon_i a_i a_j/\alpha_R$
α_{ij}	Standardized effective interaction: effective interaction between consumers i and j divided by the intraspecific effective interaction of consumer i; by definition, $\alpha_{ii} = 1$	$\alpha_{ij} = \dfrac{\alpha_{ij}^{\text{eff}}}{\alpha_{ii}^{\text{eff}}} = \dfrac{\gamma_{ij} + \varepsilon_i a_i a_j/\alpha_R}{\gamma_{ii} + \varepsilon_i a_i a_i/\alpha_R}$
ρ	Average standardized interaction: the average of the α_{ij}	$\rho = \langle\alpha_{ij}\rangle_{i\neq j} = \dfrac{1}{S(S-1)}\sum_{i\neq j}\alpha_{ij}$
$\dfrac{\sum_{i=1}^{S}C_i^*}{\langle K_i\rangle}$	Relative biomass: total biomass of the S consumers divided by their average carrying capacity	$\dfrac{\sum_{i=1}^{S}C_i^*}{\langle K_i\rangle} \approx \dfrac{S}{1+(S-1)\rho}$

of the consumer, resource abundance converges to its carrying capacity given by $K_R = r_R/\alpha_R$ (Arditi et al. 2016). Note that equation (1) differs from classical consumer-resource models (MacArthur 1972) by the presence of the γ_{ij} term; this additional parameter makes ecological sense because consumer species usually do not interact only through exploitative competition for the common resource. In the following, we refer to the term γ_{ij} as "nontrophic" interaction (note that γ_{ij} and other parameters below are interaction coefficients, but for legibility we refer only to "interaction"). In particular, this term can encapsulate positive interactions among consumers, which has already been observed in experimental settings similar to ours (Vandermeer 1969). Importantly, its presence allows all consumers to coexist on one resource (Lobry and Harmand 2006; Lobry et al. 2006). The sign convention for the γ_{ij} terms is chosen such that $\gamma_{ij} > 0$ represents a negative effect of species j on species i, while $\gamma_{ij} < 0$ is a positive effect. The intraspecific term $\gamma_{ii} > 0$ is akin to intraspecific competition of the consumers and thus must be positive (i.e., $\gamma_{ii} > 0$).

The dynamic system given by equation (1) can exhibit different behaviors, such as convergence to a fixed point or to a limit cycle. Mathematical results tend to indicate that in the presence of intraspecific competition for the consumers ($\gamma_{ii} > 0$), the system tends to converge to a fixed point (Lobry and Harmand 2006). Moreover, in the case of limit cycles, the average abundances equal the value of the fixed point (Hofbauer and Sigmund 1998, chap. 5.2). For these reasons, we base our theory only on the fixed points for which all species have positive abundances (i.e., feasible fixed points). One can, of course, directly derive the fixed point from equation (1) by equaling the brackets on the right side to zero (see app. A, sec. A2), but it is more instructive for our mechanistic understanding to transform the consumer-resource system into a dynamic model for the consumers only (MacArthur and Levins 1967; MacArthur 1970, 1972; Logofet 1992; Loreau 2010). To do so, we have to assume that the resource is at a positive equilibrium R^* and that its level adjusts faster than consumer dynamics (MacArthur 1972). We derive the resource equilibrium from its dynamic equation (1) by setting to zero the term inside the brackets:

$$R^* = \frac{1}{\alpha_R}\left(r_R - \sum_{j=1}^{S} a_j C_j\right). \tag{2}$$

By replacing the resource R with its equilibrium level R^*, the equation for the consumers' dynamics (1) follows a Lotka-Volterra type model, which describes the interactions between consumers:

$$\frac{dC_i}{dt} = C_i\left(-m_i + \varepsilon_i a_i \frac{r_R}{\alpha_R} - \sum_{j=1}^{S}\left(\gamma_{ij} + \frac{\varepsilon_i a_i a_j}{\alpha_R}\right)C_j\right). \tag{3}$$

We can identify the intrinsic growth rate of consumer i as $r_i = -m_i + \varepsilon_i a_i r_R/\alpha_R$ in the presence of the resource (i.e., it is the balance between the mortality rate m_i and the gain in fecundity from feeding on the resource $\varepsilon_i a_i r_R/\alpha_R$). We introduce the "effective interaction" $\alpha_{ij}^{\text{eff}} = \gamma_{ij} + \varepsilon_i a_i a_j/\alpha_R$, which encapsulates all interactions between consumers i and j. This effective interaction is the sum of the nontrophic interactions between consumers γ_{ij} and the term $\varepsilon_i a_i a_j/\alpha_R$ arising from exploitative competition. Note that the effective interspecific interactions can be positive or negative (due to the term γ_{ij}), while the effective intraspecific interaction is always positive ($\alpha_{ii}^{\text{eff}} = \gamma_{ii} + \varepsilon_i a_i a_i/\alpha_R > 0$). Finally, for the derivation of the BEF relationship, it is convenient to reparameterize equation (3) by making explicit the carrying capacity of the consumers:

$$\frac{dC_i}{dt} = C_i \frac{r_i}{K_i}\left(K_i - \sum_{j=1}^{S} \alpha_{ij} C_j\right), \tag{4}$$

where the parameter K_i is the carrying capacity of species i (formally, the equilibrium population size in monoculture; Arditi et al. 2016) and α_{ij} is the effective interaction between species i and species j standardized by the effective intraspecific competition of species i (see Svirezhev and Logofet 1983, p. 193; Case 2000, box 15.35):

$$\alpha_{ij} = \frac{\alpha_{ij}^{\text{eff}}}{\alpha_{ii}^{\text{eff}}} = \frac{\gamma_{ij} + \varepsilon_i a_i a_j/\alpha_R}{\gamma_{ii} + \varepsilon_i a_i a_i/\alpha_R}. \tag{5}$$

This term is composed of the strength of the exploitative competition of species j on species i ($\varepsilon_i a_i a_j/\alpha_R$) and of their nontrophic interaction (γ_{ij}); therefore, it can be seen as the standardized per capita effect of species j on species i, which we call "standardized effective interaction." Finally, the carrying capacity K_i is given by the ratio between the intrinsic growth rates r_i and the effective intraspecific competition α_{ii}^{eff}:

$$K_i = \frac{r_i}{\alpha_{ii}^{\text{eff}}} = \frac{-m_i + \varepsilon_i a_i r_R/\alpha_R}{\gamma_{ii} + \varepsilon_i a_i a_i/\alpha_R}. \tag{6}$$

Note that equations (3) and (4) are mathematically equivalent; the standardized effective interactions are in general not symmetric (i.e., $\alpha_{ij} \neq \alpha_{ji}$) and, by definition, $\alpha_{ii} = 1$.

From the consumer Lotka-Volterra model (eq. [4]), assuming no species extinction and the system being at equilibrium, one can derive the expected BEF relationship. We start by writing explicitly the system of linear equations that define the positive equilibrium densities $C_1^* > 0, \ldots, C_S^* > 0$ of model (4) (i.e., by setting the parenthesis to zero):

$$\begin{aligned} K_1 &= 1 \cdot C_1^* + \cdots + \alpha_{1S} C_S^* \\ &\vdots \quad\quad \vdots \quad\quad \vdots \\ K_S &= \alpha_{S1} C_1^* + \cdots + 1 \cdot C_S^* \end{aligned}. \tag{7}$$

We aim to obtain a general and simple equation for the BEF relationship, which involves expressing the total bio-

mass $\sum_{i=1}^{S} C_i^*$ as a function of the number of species. One possibility is to solve explicitly equation (7) for the exact biomass, but it is then not possible to extract the number of species S. Another possibility is first to sum this system of equations, which yields the following relationship between the sum of all carrying capacities, the standardized effective interactions, and the densities at equilibrium:

$$\sum_{i=1}^{S} K_i = C_1^* + \sum_{l=2}^{S} \alpha_{l1} C_1^* + \cdots + C_S^* + \sum_{l=1}^{S-1} \alpha_{lS} C_S^*. \quad (8)$$

The sum of all carrying capacities $\sum_{i=1}^{S} K_i$ gives the total densities that the system would reach in the absence of interspecific interactions among consumers. Second, one can solve equation (8) for the expected biomass. This is achieved by approximating the standardized effective interactions α_{ij} in equation (8) by their expected or average value ρ:

$$\rho = \langle \alpha_{ij} \rangle_{i \neq j} = \frac{1}{S(S-1)} \sum_{i \neq j} \alpha_{ij}. \quad (9)$$

Remember that the intraspecific standardized effective interactions are, by definition of model (4), equal to 1 ($\alpha_{ii} = 1$). We name ρ the "average standardized interaction." It follows that

$$\sum_{i \neq j} \alpha_{ij} \approx (S-1)\rho. \quad (10)$$

Finally, by placing equation (10) into equation (8), we can isolate the expected total biomass that the system will reach and, consequently, obtain the following BEF relationship:

$$\sum_{i=1}^{S} C_i^* \approx \frac{S \cdot \langle K_i \rangle}{1 + (S-1)\rho} \quad \text{or} \quad \frac{\sum_{i=1}^{S} C_i^*}{\langle K_i \rangle} \approx \frac{S}{1 + (S-1)\rho}, \quad (11)$$

where $\langle K_i \rangle$ denotes the average carrying capacity ($\langle K_i \rangle = 1/S \cdot \sum_{i=1}^{S} K_i$). The second equation is for the relative biomass (the biomass in polyculture divided by the average biomass of the species in monocultures) and not the total biomass, as customarily studied in BEF research. This expression of the BEF equation is a one-parameter model that is constrained so that it passes through the (1, 1) point. It explicitly separates the contribution of species interactions (through the average standardized interaction ρ), of the average carrying capacity $\langle K_i \rangle$, and of the number of species S on the total expected biomass $\sum_{i=1}^{S} C_i^*$. Note that standardizing the total biomass with average carrying capacity is a useful representation of the BEF relationship, as shown by Cardinale et al. (2006), because it allows for the comparison of different systems. Moreover, relative biomass naturally accounts for idiosyncratic effects due to the presence of particular competitively superior species with large carrying capacity (the selection effect). Finally, this is a one-parameter equation that depends only on ρ, which itself does not depend on intrinsic growth rates or carrying capacities (see eq. [5]). The parameter ρ can be interpreted as the "shape parameter" of the BEF relationship (see app. A, sec. A3, fig. A1; figs. A1, B1, E1, E2 are available online): a value of $\rho < 1$ gives a positive relationship, that is, the total biomass increases with species diversity; a value of $\rho > 1$ results in a negative BEF relationship, that is, the total biomass decreases with species diversity. Therefore, in order to have the strongest positive effect of species diversity on the total biomass, the amount of average standardized interaction (ρ) has to be as low as possible.

It is worth mentioning that equations similar to the BEF model (eq. [11]) have been derived independently and from different perspectives at least four other times (Vandermeer 1970; Wilson et al. 2003; Cardinale et al. 2004; Fort 2018). Vandermeer (1970) explored the question of the number of species coexisting at equilibrium in communities of competing species. He derived an equation for the expected density (his eq. [3]) that can be easily identified in our equation (11) except that it contains an additional covariance term between the interaction coefficients and the equilibrium density of the species. This correction term accounts for cases where, for example, species with high equilibrium density have large interaction coefficients. However, including this covariance term makes the equation not solvable for the expected density, and Vandermeer (1970) assumed that it was negligible. Wilson et al. (2003) used mean-field approximation to derive several key features of community structure (e.g., species abundance distributions) for Lotka-Volterra systems. Their equation (5a) for the mean "target density" is also easily identified in our equation (11); their equation was used specifically as a BEF relationship by Rossberg (2013). Cardinale et al. (2004) specifically studied the effect of species diversity on total primary productivity and again developed an equation (their eq. [7]) similar to our model (11), although in the more restrictive case of identical carrying capacities. In comparison, our derivation of the BEF model (11), as well as that in Fort (2018), were explicitly intended for modeling how relative biomass (and not total biomass) scales with species richness S. Note that the results of the meta-analysis of Fort (2018) show that a correction by a covariance term appears not necessary.

That five independent derivations converge toward similar equations provides support for equation (11) as a representation of a well-grounded model for the BEF relationship. Interestingly, it also receives empirical support from the meta-analysis of Cardinale et al. (2006; see their fig. 2*a*). In this work, the fit of three statistical models (log, power, and hyperbolic) were compared for the relationship between relative biomass Y (exactly similar to the left term of the second eq. [11]) and species richness S in a data set of 45 studies.

It was found that the hyperbolic Michaelis-Menten equation was the best model for the majority of studies. They fitted the following equation: $Y = Y_{\max}S/(K + S)$, with $Y_{\max}$ being the asymptote and K being the half-saturation constant (the value of S for which half of $Y_{\max}$ is attained). We can easily see that our equation (11) corresponds to a Michaelis-Menten equation, with the parameter $Y_{\max}$ identified as ρ^{-1} and K as $\rho^{-1} - 1$ (here, K is the half-saturation parameter and not the carrying capacity). Note that in their representation $Y_{\max}$ and K are not independent since, by definition, $Y = 1$ for $S = 1$, and therefore $Y_{\max} = K + 1$ (the estimated values for the parameters $Y_{\max}$ and K shown in the right panel of fig. 2*a* in Cardinale et al. [2006] are perfectly compatible with this constraint). First, the BEF model provides a mechanistic justification for the use of the Michaelis-Menten model (with the constraint on the parameters). Second, equation (11) gives a biological explanation for the asymptote ($Y_{\max}$) as the inverse of the average standardized interaction ρ in the community.

Including Temperature in the BEF Model

The second step is to include the effect of temperature on the interaction strength and the demographic parameters and then to examine its consequences for the BEF relationship. According to theory and empirical data (Rall et al. 2010; Englund et al. 2011; Gilbert et al. 2014), in the rising part of a thermal performance curve (Dowd et al. 2015) the mortality, growth, and attack rates of ectothermic species increase with temperature. Therefore, in the consumer-resource system given by equation (1), these rates are assumed to increase with temperature. Following empirical evidence (Rall et al. 2010), we assume conversion efficiencies ε_i to be unaffected by temperature; for simplicity and in the absence of empirical evidence, the nontrophic interactions among consumers (γ_{ij}) and the intraspecific competition of the resource (α_R) were also assumed to be unaffected. In the rising part of a thermal performance curve, temperature-dependent parameters follow the general functional form $\exp(-E/(k \cdot T))$, where E is the activation energy, k is the Boltzmann constant, and T is the absolute temperature in kelvins (Englund et al. 2011; Gilbert et al. 2014).

We can then examine the temperature dependence of the standardized effective interaction. By making explicit the temperature dependence of the parameters in equation (5), we obtain

$$\alpha_{ij}(T) = \frac{\gamma_{ij} + \exp\left(-\frac{2E_a}{k \cdot T}\right)A_{ij}}{\gamma_{ii} + \exp\left(-\frac{2E_a}{k \cdot T}\right)A_{ii}}, \tag{12}$$

where A_{ij} represents the exploitative competition for the common resource(s), which is given by $A_{ij} = \varepsilon_i a_i a_j/\alpha_R$ (E_a is the activation energy of the attack rate). The derivative of the interspecific interaction coefficients with respect to temperature is given by

$$\frac{d\alpha_{ij}(T)}{dT} = \frac{A_{ij}\gamma_{ii} - A_{ii}\gamma_{ij}}{\left(\gamma_{ii} + \exp\left(-\frac{2E_a}{k \cdot T}\right)A_{ii}\right)^2}\exp\left(-\frac{2E_a}{k \cdot T}\right) \cdot \frac{2E_a}{kT^2}. \tag{13}$$

All parts of the right-hand side of equation (13) are trivially positive except for the numerator. The A_{ij} and A_{ii} terms are positive, but there is no biological reason to expect that one term is consistently larger than the other. This is, however, not the case for the nontrophic interaction terms γ, for which γ_{ii} is expected to be generally larger than γ_{ij} in a community with no extinction. We could expect some large interspecific terms (Connell 1983), but the vast majority must be weak for the system to persist, especially when species richness increases. As a consequence, the numerator is expected to be positive, and thus the average standardized interaction ρ increases with temperature.

Figure 1 illustrates this phenomenon for an arbitrary set of six species and one discrete resource. For this figure, the attack rates have been chosen as $a_1 = 0.08$, $a_2 = 0.144$, $a_3 = 0.208$, $a_4 = 0.272$, $a_5 = 0.336$, $a_6 = 0.4$, $\gamma_{ii} = 1$, and $\gamma_{ij} = 0$, and the activation energy was set to $E = 0.55$ [eV] according to Gilbert et al. (2014). Figure 1*A* shows that the attack rate increases as a function of temperature. As a consequence, from equation (12) the standardized effective interactions between consumers also increases (fig. 1*B*). Finally, from equation (11) we can deduce that the BEF relationship becomes flatter with increasing average standardized interaction ρ as a consequence of increasing temperature (fig. 1*C*). The theory presented in this figure is robust to changes in parameter values as well as to using multiple resources or a continuous resource axis. The mathematical reason behind this robustness is that, by increasing the attack rate (or the amplitude of the niche utilization function), the interspecific standardized effective interactions increase, in general, until some saturation occurs.

Similarly, we can study the effect of temperature on consumer carrying capacity. By making explicit the temperature dependence of the parameters in the carrying capacity (eq. [6]), we obtain

$$K_i(T) = \frac{-\exp\left(-\frac{E_m}{k \cdot T}\right)m_i + \exp\left(-\frac{(E_a + E_r)}{k \cdot T}\right)\varepsilon_i a_i r_R/\alpha_R}{\gamma_{ii} + \exp\left(-\frac{2E_a}{k \cdot T}\right)a_i a_i \varepsilon_i/\alpha_R}, \tag{14}$$

where E_m, E_r, and E_a are the activation energy for the mortality, resource growth rate, and attack rates, respectively. Then the derivative relative to the temperature is given by

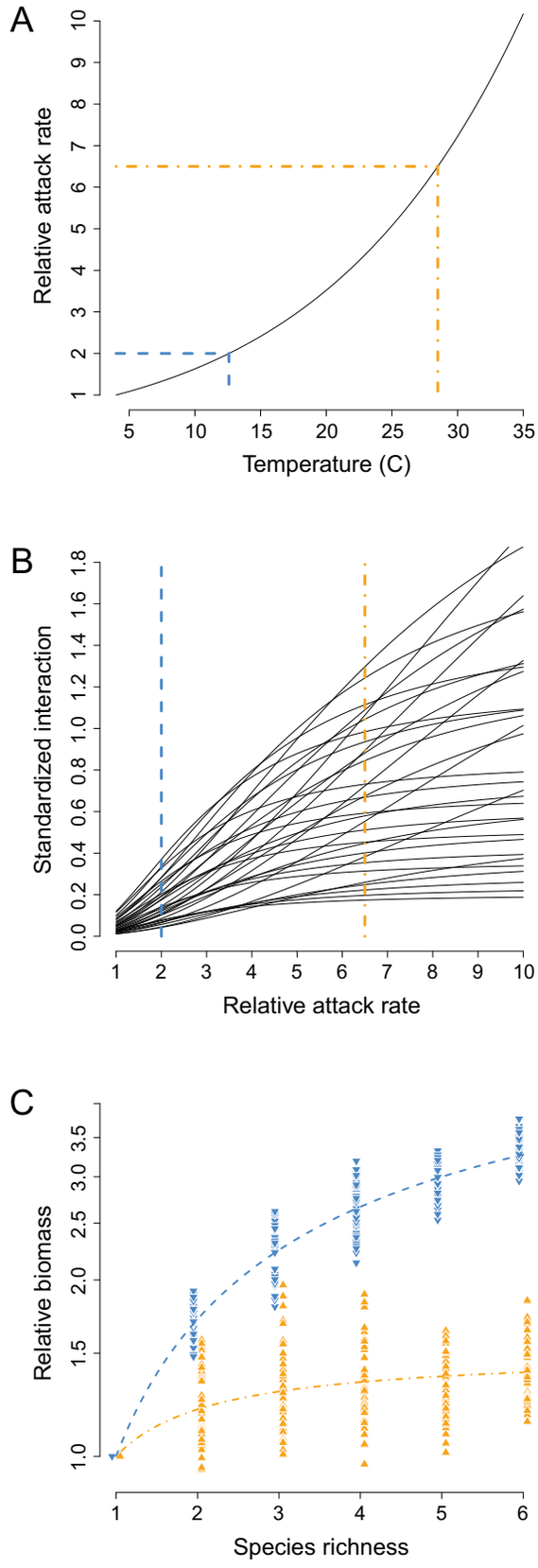

$$\frac{dK_i(T)}{dT} = \frac{1}{kT^2}\cdot\left[\frac{-\exp\left(-\frac{E_m}{k\cdot T}\right)m_iE_m + \exp\left(-\frac{(E_a+E_r)}{k\cdot T}\right)\varepsilon_i a_i r_R E_a/\alpha_R}{\gamma_{ii} + \exp\left(-\frac{2E_a}{k\cdot T}\right)a_i a_i \varepsilon_i/\alpha_R} - \frac{\left(\left(-\exp\left(-\frac{E_m}{k\cdot T}\right)m_i + \exp\left(-\frac{(E_a+E_r)}{k\cdot T}\right)\varepsilon_i a_i r_R/\alpha_R\right)\times \exp\left(-\frac{2(E_a+E_r)}{k\cdot T}\right)a_i a_i 2E_a\varepsilon_i/\alpha_R\right)}{\left(\gamma_{ii} + \exp\left(-\frac{2(E_a+E_r)}{k\cdot T}\right)a_i a_i \varepsilon_i/\alpha_R\right)^2}\right]. \quad (15)$$

Contrary to equation (13), the sign of the term inside the brackets mainly depends on the balance between temperature-dependent mortality and fecundity, which cannot be unambiguously determined. Therefore, the carrying capacity may increase or decrease with temperature.

Global warming is not only about an increase in the average temperature; it is also predicted that variation in temperature will increase. For the same temperature average, an increase in variation will also increase the average attack rate (fig. B1). This is a consequence of the convexity of the attack rate curve (fig. 1*A*). Therefore, an increase in temperature variation results in an increase in average interspecific interaction, and consequently it will further flatten the BEF relationship.

Material and Methods

To empirically study the effect of temperature on the BEF relationship, we used the natural community inhabiting the rainwater-filled leaves of the carnivorous plant *Sarracenia purpurea* (Addicott 1974; Karagatzides et al. 2009). We chose natural microcosms because they have been shown to be valuable tools to address larger-scale ecological questions (Sri-

Figure 1: Theoretical effects of temperature on the attack rates, standardized effective interactions, and the biodiversity–ecosystem functioning (BEF) relationship. *A*, In the rising part of the performance curve, the attack rate increases with temperature (Englund et al. 2011; Gilbert et al. 2014; blue dashed lines: 12.5°C; orange dashed-dotted lines: 28.5°C). The range of temperature was chosen to correspond with the physiological range of the protozoan morphospecies used in the present study according to empirical data. *B*, Consequence of attack rate increase on the standardized effective interactions α_{ij} in a community of six species (see the text for parameter details). Lines represent the α_{ij} for each pair of species as a function of attack rate. *C*, Effect of an increase in temperature—and therefore of average interspecific interaction—on the BEF relationship of hypothetical communities. The three panels illustrate that an increase in temperature translates into an increase in attack rate, which in turn induces larger standardized effective interactions and ultimately flattens the BEF relationship.

vastava et al. 2004). In Europe, this community lacks the complexity of its North American counterpart (Kneitel and Miller 2002; Zander et al. 2016) and is generally composed of only two trophic levels. Bacteria form the lower trophic level and utilize the nutrients of the insects that they decompose. These bacteria act as the prey for the protozoans and rotifers in the second trophic level. The concise consumer-resource relationship of the European *S. purpurea* community makes it perfectly suited to our modeling framework: it is simple enough to render negligible the possible effects of processes known to affect the BEF relationship in larger systems (see Tilman et al. 2014) while keeping competitive interactions as a key process for community dynamics (Vandermeer 1969). In addition, *S. purpurea* is located along a large temperature/altitude gradient within Switzerland, but the same common protozoan morphospecies can still be found in communities across this gradient (Parain et al. 2016). This feature allows for experiments to be conducted with protozoans of similar morphotype but that have naturally experienced different local temperature conditions, which is ideal for addressing how temperature will affect the BEF relationship.

The protozoan species used in our experiment were collected from two sites in Switzerland differing in temperature: Les Tenasses (cold site; elevation, 1,200) and Champ Buet (warm site; elevation, 500 m). At each site and on the same day, we marked 50 leaves that were close to opening. Two weeks later, we returned to the two field sites and used a sterilized pipette to collect the rainwater from these now-opened leaves. The samples from each field site were pooled together in an autoclaved Nalgene bottle (one bottle per field site) and were transported on ice to the laboratory. This rainwater contained the protozoans (consumers) and bacteria (resources) that would be used in the experiment. By collecting water at both sites on the same day and from the leaves of the same cohort, we could ensure that the communities at both sites were from the same successional stage.

For each site, six protozoan morphospecies (three flagellates and three ciliates) that were morphologically similar between the two sites were isolated into monocultures (see app. C for more details). We then conducted a laboratory experiment in which three temperature treatments were crossed with protozoan diversity levels (one, two, four, and six species). The daily minimum, average, and maximum June temperatures are, respectively, 7.5°, 10.3°, and 18.3°C for the cold site and 10°, 15.5°, and 20.9°C for the warm site. These temperatures were used to program incubators that mimicked natural temperature fluctuations at both sites. Three incubators for each site were programmed to represent (1) the local conditions (treatment *lc*) of the site for the month of June, (2) an increased average temperature by 5°C (treatment *t5*) while maintaining the same daily variation as in treatment *lc* (amplitude of 10°C), and (3) an increase in average temperature by 5°C and in variation (amplitude of 20°C; treatment *hv*). The temperature programs had incremental increases and decreases in temperature over a 24-h time period according to methods used in Gray et al. (2016). We chose the experimental highest temperatures so that they fell inside the temperature range experienced by the communities in the field, which was measured by data loggers placed inside leaves at both sites during an entire season (see Zander et al. 2017).

Within these three temperature treatments, the protozoans were grown either in monoculture (five replicates for a total of 180 observations) or in communities of two, four, or six morphospecies (four replicates for a total of 216 observations; see table C1; tables C1, D1, D2, E1–E6 are available online). We ran the experiment for 6 days and determined the biomass of each morphospecies every 2 days. In our analyses, we used the biomasses on the last day, when protozoans reached a steady state (see Kadowaki et al. 2012). A detailed description of the procedure used in the experiment is given in appendix C.

We used nonlinear regression to estimate the average standardized interaction ρ (eq. [11]) from our experimental results. A priori, ρ may vary with the number of species. Moreover, if facilitation occurs (i.e., negative effective interactions), ρ may take negative values. In this case, to avoid divergence ρ must increase with the number of species and must tend asymptotically toward positive values. Indeed, in a linear Lotka-Voltera model (like in our eq. [4]) the strength of facilitation must decrease with an increasing number of species to avoid mathematical singularities (for details, see app. A, sec. A3). Therefore, we used two parameterizations for ρ. The first and simplest case assumes ρ to be constant: $\rho \sim \lambda_1$, with $\lambda_1 > 0$. The second parameterization is given by $\rho \sim \lambda_1 - \lambda_2/S$, with λ_1 and $\lambda_2 > 0$; it is designed to account for facilitation, allowing ρ to take negative values in species-poor communities, and to tend asymptotically to the positive value λ_1. We fitted the two parameterizations and selected the most parsimonious model according to the Bayesian information criterion.

Results

The experimental results met the theoretical expectations. Figure 2 shows how temperature affected the BEF relationship for the relative biomass of protozoans from natural communities. When protozoans were grown at their local temperature (*lc* treatment), both BEF relationships were positive, with a clear case of positive interactions for the cold site (i.e., relative biomass is larger than species numbers). With an average increase of 5°C, this relationship remained positive at both sites but, as predicted, with a lower slope compared with the *lc* treatment. Finally, with an increased temperature and an increased variability in temperature (*hv* treatment), the BEF relationship became flatter for the cold site and even negative

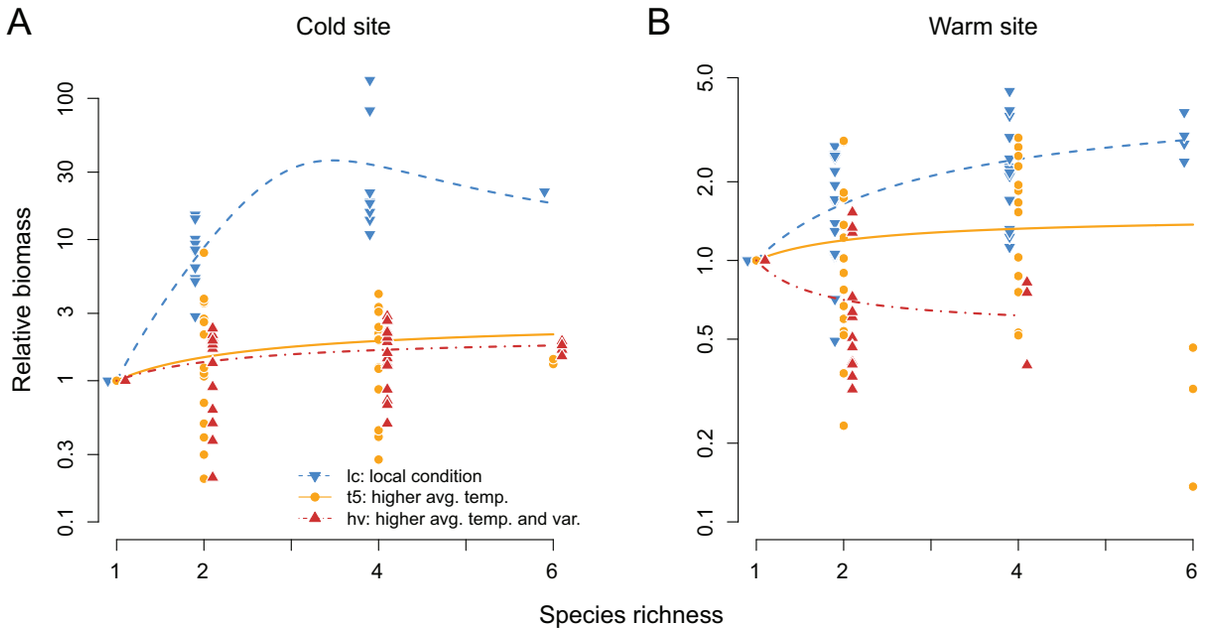

Figure 2: Experimental results for the effects of temperature change on the biodiversity–ecosystem functioning (BEF) relationship. *A*, Cold site (average temperature, 10.3°C). *B*, Warm site (average temperature, 15.5°C). The blue triangles represent the communities growing at their site temperature (*lc*), the orange circles represent those growing at the temperature average increased by 5°C (*t5*), and the red triangles represent those growing at the temperature average and variation increased by 5° and 10°C, respectively (*hv*). For better visualization, all data points are shifted slightly to the right so that the symbols for the temperature treatments do not overlap. The lines represent the fits of the mechanistic BEF relationship (eq. [11]), where the average standardized interaction ρ was modeled as either constant or dependant on the number of species. Note that positive interactions were observed among protozoans from the cold site that grew at their local temperature (*A*) and that some species became extinct in the six-species communities in the *hv* treatment (*B*). This figure shows that, at both sites, warming results in a flattening of the BEF relationship, which is in accordance with the theoretical model.

for the warm site (Stachová and Lepš 2010; Rychtecká et al. 2014).

The fitted values for the average standardized interaction (λ_1) revealed a systematic increase with increased temperature average and/or variation (tables 2, 3). This is perfectly in line with the theoretical predictions that the slope of the BEF relationship becomes flatter and even negative with increased temperature average and/or variation. Note that the differences in λ_1 values among the temperature treatments for the cold site are not statistically significant (*lc* vs. *t5*, $P = .770$; *lc* vs. *hv*, $P = .182$; *t5* vs. *hv*, $P = .443$; *t*-test with Holm-Bonferroni-corrected *P* values), while they are significant for the warm site (*lc* vs. *t5*, $P = .002$; *lc* vs. *hv*, $P < .001$; *t5* vs. *hv*, $P = .003$).

Figure 3 shows the effect of increased average temperature and temperature variation on the average carrying capacity of each of the consumer species. This figure illustrates that the carrying capacity can either increase or decrease with increased temperature average and/or variation, as expected from equation (15). Figure 4 shows the effect of temperature on the total biomass (fitted values are given in table D2). It displays the combined effect of temperature on the slope and on the carrying capacity of the BEF relationship; the main difference with figure 2 resides in the variable intercepts (corresponding to the average carrying capacities), which, by definition, equals 1 with the relative biomass. Although the average carrying capacity is variable, the average standardized interaction ρ will generally increase with temperature, and thus the BEF relationship will flatten, as theoretically predicted. Data and the R code are deposited in the Dryad Digital Repository: https://dx.doi.org/10.5061/dryad.hk1h26n (Parain et al. 2018).

We observed several cases of species extinctions in our experiment (in 40 of 396 communities). These cases were not included in the statistical analyses of the BEF relationship, since our model was developed for situations where no extinction occurs. For completeness, we checked whether our conclusions would change if we included the cases with extinctions in the analyses, and we found that our results remained valid (see app. E). We performed logistic regressions at the warm site and the cold site on the frequency of extinctions as a function of temperature treatment and spe-

Table 2: Comparisons of the Akaike information criterion (AIC) and the Bayesian information criterion (BIC) for the two models of the average standardized interaction in the biodiversity–ecosystem functioning (BEF) relationship

Site, temperature treatment	Model: $\rho \sim \lambda_1$		Model: $\rho \sim \lambda_1 - \lambda_2/S$	
	AIC	BIC	AIC	BIC
Cold:				
lc	245.8	248.3	237.8	**241.4**
t5	134.7	**138**	132.7	137.2
hv	76.2	**79.3**	78.2	82.8
Warm:				
lc	91.1	**94.3**	93.1	97.6
t5	83.9	**86.8**	85.6	90.0
hv	17.1	**18.7**	19.1	21.4

Note: The BIC values for the best model are in boldface type. Note that the BIC values of the two models for the *t5* treatment at the cold site are very similar (ΔBIC = 0.3). For this treatment, we chose the simplest model despite a slightly larger BIC value. Note that in the analyses for the total biomass (fig. 4; table D1), the support for the simplest model in this treatment was stronger. *hv* = temperature increase by 5°C and higher daily temperature variation; *lc* = local temperature; *t5* = temperature increase by 5°C.

cies number. Extinction probability consistently increased with species richness, but the results were inconclusive with temperature treatment.

Discussion

Both our empirical and theoretical results show that the BEF relationship flattens with increased temperature and temperature variation. The mechanistic explanation for these results is a temperature-induced increase in attack rates (or increased amplitude of the niche utilization functions in the case of continuous resources), which translates into higher effective interactions and ultimately in higher average ρ. Although we did not measure attack rates in our experiment, the increase in attack rate with rising temperature has received empirical support (Rall et al. 2010; Englund et al. 2011; Gilbert et al. 2014). This mechanism is induced by a basic increase in metabolic rate with temperature. It is thus very general and should apply to most natural ecosystems composed of nonhomeothermic species experiencing the rise in average temperature and variation predicted by climate change models (IPCC 2014).

The potential generalizability of our results has already been demonstrated experimentally in algal systems (Steudel et al. 2012) and in grassland communities (De Boeck et al. 2007, 2008). Both studies experimentally found a temperature-induced negative effect on the BEF relationship, but the ability to determine the underlying mechanism behind this result remained a challenge. Steudel et al. (2012) highlighted the need to theoretically examine the effect of stress intensity on the BEF relationship. Our study was able to accomplish this for one key driver of the BEF relationship and for one key environmental stressor, namely, interspecific interaction and temperature, respectively. Our model shows that these two stressors are in fact not independent but linked by a basic metabolic mechanism. The next step would be to incorporate additional abiotic stressors, as climate change will likely alter these abiotic stressors directly or indirectly, which can influence the way productivity and species richness are interrelated (Grace et al. 2016). To our knowledge, although several experimental studies have considered the effect of abiotic stressors on the BEF relationship (Cd pollution, Li et al. 2010; e.g., Mulder et al. 2001), only one study has experimentally investigated a stressor (salinity) in combination with temperature (Steudel et al. 2012). The relative impact of interaction-mediated vs. other drivers on the BEF relationship under climate change thus remains an important research area for mitigating the effects of global changes on ecosystem functioning.

Interestingly, of the studies that examined nontemperature environmental stressors found that positive interactions between the species were likely to occur in the stressed environment, which counteracted the potential negative impact on the BEF relationship (Mulder et al. 2001; Li et al. 2010). We also detected a case that was clearly indicative of positive interactions; however, it occurred in the local conditions treatment *lc* at the cold site (fig. 2*A*, blue line). Here, the total biomass was larger than the sum of the carrying capacities, or equivalently the relative biomass was larger than the number of species (see, e.g., Vandermeer 1969; DeLong and Vasseur

Table 3: Estimated parameters of the best model in table 2 for the biodiversity–ecosystem functioning (BEF) relationship

Site, temperature treatment, parameter	Estimate	SE	*P*
Cold:			
lc: λ_1	.186	.157	<.001
lc: λ_2	1.915	.629	.002
t5: λ_1	.363	.130	<.001
hv: λ_1	.475	.070	<.001
Warm:			
lc: λ_1	.213	.036	<.001
t5: λ_1	.675	.139	.002
hv: λ_1	1.830	.367	.002

Note: For each treatment, the best model was given by $\rho \sim \lambda_1$, except for communities from the cold site that were subjected to the local conditions (*lc*) temperature treatment. In this case, positive interactions were observed (fig. 2*A*), and the appropriate model was given by $\rho \sim \lambda_1 - \lambda_2/S$. For the parameter λ_1, the *P* values (two tailed) test the null hypothesis (H_0) that $\lambda_1 = 1$, while for λ_2 the null hypothesis (H_0) is $\lambda_2 = 0$. Rejecting the null hypothesis for λ_1 implies that it is statistically significantly smaller than 1 (positive BEF relationship) or significantly larger than 1 (negative BEF relationship). Rejecting the null hypothesis for $\lambda_2 > 0$ implies positive interactions among consumers.

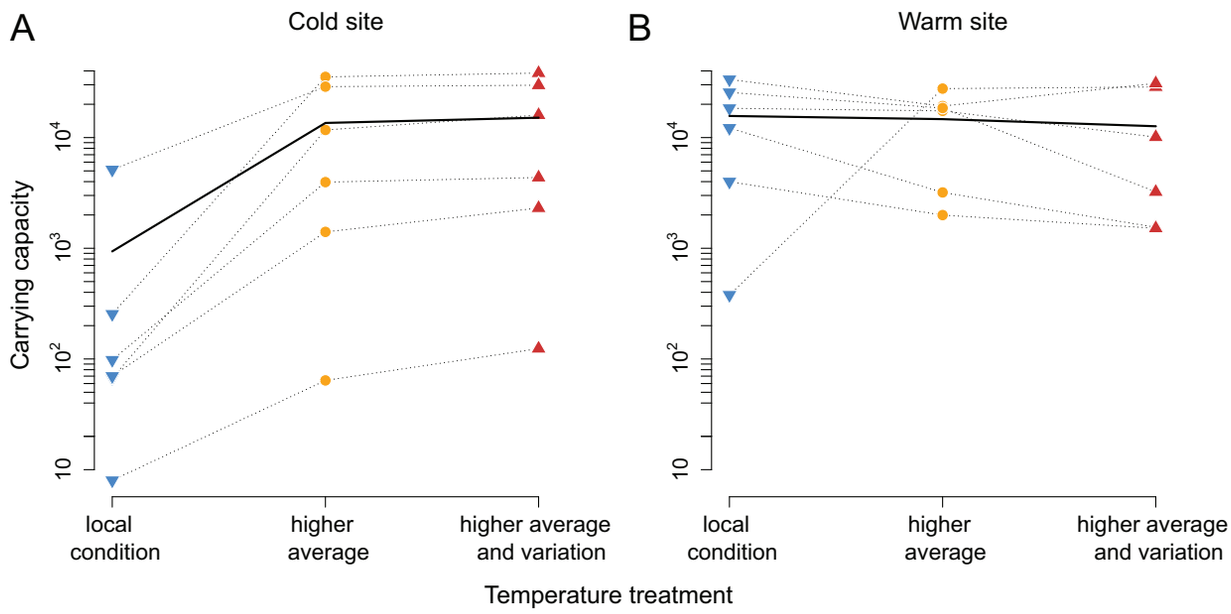

Figure 3: Effects of increased temperature on the average carrying capacity (biomass in monoculture) of each species from the two sites. *A*, Symbols represent the average ($n = 5$) carrying capacity of each species from the cold site in the different temperature treatments. The average carrying capacity of the six species is represented by the solid black line, which shows that it increases in the *t5* (orange circles) and *hv* (red triangles) treatments compared with the *lc* treatment (blue triangles). *B*, Same as *A*, but for the warm site. Here, the average carrying capacity of a community in the *t5* and *hv* treatments is almost constant, but the species-specific carrying capacities show idiosyncratic responses. *hv* = higher average temperature and variation; *lc* = local conditions; *t5* = high temperature.

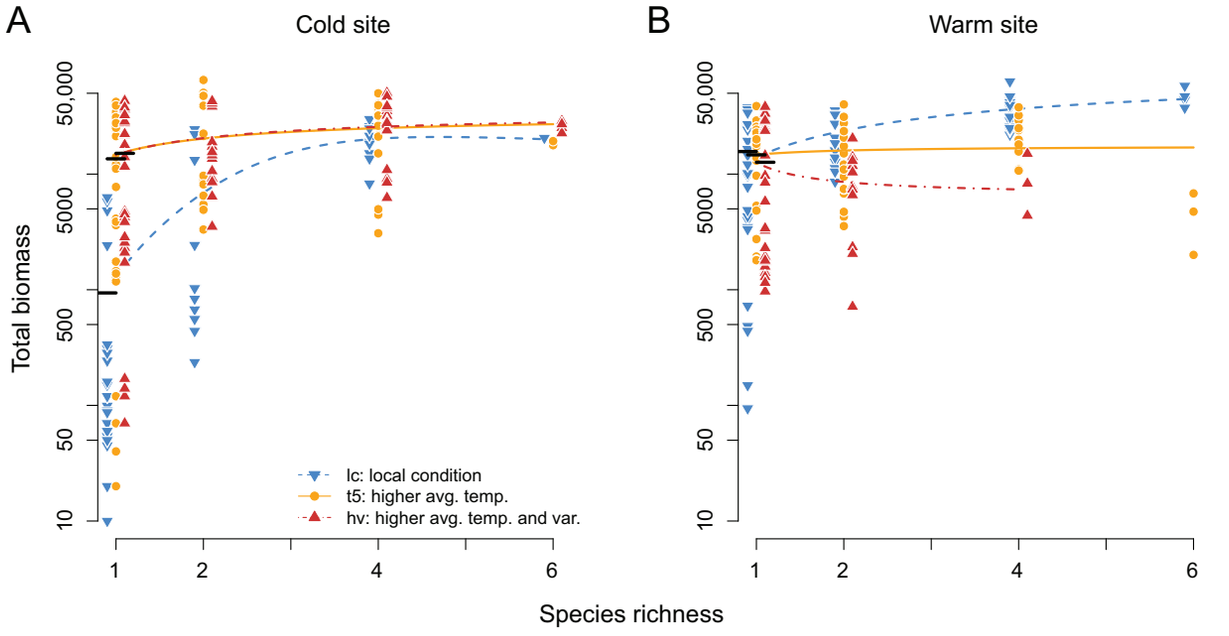

Figure 4: Experimental results of the effects of temperature change on the total biomass and its relationship with species richness. Symbols are the same as figure 2. This figure shows that at the cold site, the average carrying capacity (i.e., total biomass when species are grown in monoculture, whose averages are given by the black dashes; dashes and symbols are slightly shifted for better visualization) increases with global warming, while it remains constant at the warm site. The slopes of the biodiversity–ecosystem functioning relationships are qualitatively similar to those in figure 2 and consistently decrease with increased temperature and temperature variation.

2012). We checked whether the presence of particular combinations of morphospecies was prevalent in our experimental microcosms where facilitation was evident, but we found no clear candidates. Positive interactions in protozoan communities have not been well studied, and more investigation is required to uncover the mechanisms underlying this phenomenon. For instance, the consumption of deleterious prey by a specialized species or the release of some beneficial secondary products could bolster the growth of the protozoan community. As a consequence, at least some of the interspecific nontrophic interaction terms γ_{ij} of equations (1) and (3) should be negative. Modeling facilitation in communities requires the dampening of interaction coefficients to prevent the system from expanding to infinity (Goh 1979; Rohr et al. 2014). Without precise knowledge of the process, we adopted a general modeling framework that provides a reasonable fit to the way the average interspecific interaction ρ is dependent on the number of species S (see app. A, sec. A3). Yet in accordance with the experimental results of Mulder et al. (2001) and Li et al. (2010), the potential effect of positive interactions to lessen the impact of multiple abiotic stressors on the BEF relationship should be further investigated.

We based our theoretical arguments on a classical Lotka-Volterra competition model that assumes the dynamics of the common resources to be faster than that of the consumers. With this approach, a better mechanistic understanding of exploitative competition can be reached. However, it is important to realize that the assumption of "fast" resources is not critical for our theory (see app. A, sec. A2). In fact, it is sufficient that the system goes to an equilibrium or to limit cycles (the population average under limit cycles in a Lotka-Volterra model equals the value of the interior equilibrium point; Hofbauer and Sigmund 1998, chap. 5.2). Another critique can be raised from the choice of framing our model within a limited temperature range, namely, in the rising part of the thermal performance curve. First, it is difficult to develop a general theory because of the nonmonotonicity occurring when passing the thermal maximum. Second, because the decrease in performance beyond the thermal maximum is quite abrupt (Vasseur et al. 2014), we expect extinctions to occur because of negative intrinsic growth rates ($r_i < 0$). In this situation, a BEF theory becomes meaningless.

Our approach is based on relative biomass, while the usual currency in BEF studies is the total biomass (Loreau 2010). The main difference resides in the average level of biomass in monocultures (i.e., the average carrying capacity $\langle K_i \rangle$), which can be highly variable with total biomass (see, e.g., Steudel et al. 2012), while by definition it equals 1 with relative biomass. With increasing temperature, we found that average carrying capacity increases, remains constant, or decreases (fig. 3). These different responses can be understood by the fact that the sign of the mathematical expression for the carrying capacity (eq. [15]) depends on the exact balance between the temperature-dependent parameters. In contrast, the average standardized interaction ρ will generally increase with temperature, and thus the BEF relationship will decrease. Note that relative biomass (eq. [11]) accommodates the idiosyncratic response of the carrying capacity (the selection effect), which suggests that this measure is a natural currency for the BEF relationship that allows cross-system comparisons (Cardinale et al. 2006). In our case, the benefit of using relative biomass can be evaluated by comparing figures 2 and 4. While the results are qualitatively equivalent to those with relative biomass, the fitted curves in figure 4 are more difficult to interpret because of the variability and temperature dependency of the biomasses in monocultures.

Our results are a crucial first step toward understanding and predicting the effects of climate change on the BEF relationship. The results are key, as they provide evidence that protecting a high level of biodiversity will not be a guarantee for high ecosystem functioning, and thus they contribute to the arguments for mitigating climate change. Future experiments should investigate the impact of temperature increase on community dynamics by directly measuring attack rate and interaction coefficients. Another aspect that deserves more attention is that species extinction will become more frequent with global warming, not only because interspecific competition increases but also because species may ultimately live at the edge or even cross over their physiological boundaries (Petchey et al. 1999; Vasseur et al. 2014). An open question in this respect is the role of temperature as a factor for natural selection. Thus, future research must include species extinctions in both an ecological framework and an evolutionary framework.

Acknowledgments

We are grateful to Christian Mazza, Avril Weinbach, and Nicolas Loeuille for insightful discussions. We thank the Direction générale de l'environnement of the Canton de Vaud for authorization to sample in protected areas. Funding was received from the Swiss National Science Foundation (SNSF; grant 31003A_138489 awarded to L.-F.B). We have no competing interests.

Statement of authorship: E.C.P., S.M.G., and L.-F.B. designed the experiment; E.C.P. conducted the experiment; R.P.R. developed the theoretical part; E.C.P., R.P.R., and L.-F.B. performed statistical analyses; E.C.P. and R.P.R. wrote the first draft; and all authors contributed to writing the final manuscript.

Literature Cited

Addicott, J. F. 1974. Predation and prey community structure: an experimental study of the effect of mosquito larvae on the protozoan communities of pitcher plants. Ecology 55:475–492.

Arditi, R., L.-F. Bersier, and R. P. Rohr. 2016. The perfect mixing paradox and the logistic equation: Verhulst vs. Lotka. Ecosphere 7:e01599.

Cardinale, B. J., A. R. Ives, and P. Inchausti. 2004. Effects of species diversity on the primary productivity of ecosystems: extending our spatial and temporal scales of inference. Oikos 104:437–450.

Cardinale, B. J., K. L. Matulich, D. U. Hooper, J. E. Byrnes, E. Duffy, L. Gamfeldt, P. Balvanera, M. I. O'Connor, and A. Gonzalez. 2011. The functional role of producer diversity in ecosystems. American Journal of Botany 98:572–592.

Cardinale, B. J., M. A. Palmer, and S. L. Collins. 2002. Species diversity enhances ecosystem functioning through interspecific facilitation. Nature 415:426–429.

Cardinale, B. J., D. S. Srivastava, J. E. Duffy, J. P. Wright, A. L. Downing, M. Sankaran, and C. Jouseau. 2006. Effects of biodiversity on the functioning of trophic groups and ecosystems. Nature 443:989–992.

Case, T. J. 2000. An illustrated guide to theoretical ecology. Oxford University Press, New York.

Connell, J. H. 1983. On the prevalence and relative importance of interspecific competition: evidence from field experiments. American Naturalist 122:661–696.

De Boeck, H. J., C. M. H. M. Lemmens, B. Gielen, H. Bossuyt, S. Malchair, M. Carnol, R. Merckx, R. Ceulemans, and I. Nijs. 2007. Combined effects of climate warming and plant diversity loss on above- and below-ground grassland productivity. Environmental and Experimental Botany 60:95–104.

De Boeck, H. J., C. M. H. M. Lemmens, C. Zavalloni, B. Gielen, S. Malchair, M. Carnol, R. Merckx, J. Van den Berge, R. Ceulemans, and I. Nijs. 2008. Biomass production in experimental grasslands of different species richness during three years of climate warming. Biogeosciences 5:585–594.

Dell, A. I., S. Pawar, and V. M. Savage. 2011. Systematic variation in the temperature dependence of physiological and ecological traits. Proceedings of the National Academy of Sciences of the USA 108: 10591–10596.

DeLong, J. P., and D. A. Vasseur. 2012. Coexistence via resource partitioning fails to generate an increase in community function. PLoS ONE 7:e30081.

Dowd, W. W., F. A. King, and M. W. Denny. 2015. Thermal variation, thermal extremes and the physiological performance of individuals. Journal of Experimental Biology 218:1956.

Englund, G., G. Ohlund, C. L. Hein, and S. Diehl. 2011. Temperature dependence of the functional response. Ecology Letters 14:914–921.

Fort, H. 2018. Quantitative predictions from competition theory with an incomplete knowledge of model parameters tested against experiments across diverse taxa. Ecological Modelling 368:104–110.

Gilbert, B., T. D. Tunney, K. S. McCann, J. P. DeLong, D. A. Vasseur, V. Savage, J. B. Shurin, et al. 2014. A bioenergetic framework for the temperature dependence of trophic interactions. Ecology Letters 17:902–914.

Goh, B. S. 1979. Stability in models of mutualism. American Naturalist 113:261–275.

Grace, J. B., T. M. Anderson, E. W. Seabloom, E. T. Borer, P. B. Adler, W. S. Harpole, Y. Hautier, et al. 2016. Integrative modelling reveals mechanisms linking productivity and plant species richness. Nature 529:390–393.

Gray, S. M., T. Poisot, E. Harvey, N. Mouquet, T. E. Miller, and D. Gravel. 2016. Temperature and trophic structure are driving microbial productivity along a biogeographical gradient. Ecography 39:981–989.

Hector, A., B. Schmid, C. Beierkuhnlein, M. C. Caldeira, M. Diemer, P. G. Dimitrakopoulos, J. A. Finn, et al. 1999. Plant diversity and productivity experiments in European grasslands. Science 286:1123–1127.

Hofbauer, J., and K. Sigmund. 1998. Evolutionary games and population dynamics. Cambridge University Press, Cambridge.

Hooper, D. U., E. C. Adair, B. J. Cardinale, J. E. K. Byrnes, B. A. Hungate, K. L. Matulich, A. Gonzalez, J. E. Duffy, L. Gamfeldt, and M. I. O'Connor. 2012. A global synthesis reveals biodiversity loss as a major driver of ecosystem change. Nature 486:105–108.

Hooper, D. U., F. S. Chapin, J. J. Ewel, A. Hector, P. Inchausti, S. Lavorel, J. H. Lawton, et al. 2005. Effects of biodiversity on ecosystem functioning: a consensus of current knowledge. Ecological Monographs 75:3–35.

IPCC (Intergovernmental Panel on Climate Change). 2014. Climate change 2014: mitigation of climate change. Cambridge University Press, Cambridge.

Kadowaki, K., B. D. Inouye, and T. E. Miller. 2012. Assembly-history dynamics of a pitcher-plant protozoan community in experimental microcosms. PLoS ONE 7:e42651.

Karagatzides, J. D., J. L. Butler, and A. M. Ellison. 2009. The pitcher plant *Sarracenia purpurea* can directly acquire organic nitrogen and short-circuit the inorganic nitrogen cycle. PLoS ONE 4:e6164.

Kneitel, J. M., and T. E. Miller. 2002. Resource and top-predator regulation in the pitcher plant (*Sarracenia purpurea*) inquiline community. Ecology 83:680–688.

Li, J.-T., H.-N. Duant, S.-P. Li, J.-L. Kuang, Y. Zeng, and W.-S. Shu. 2010. Cadmium pollution triggers a positive biodiversity-productivity relationship: evidence from a laboratory microcosm experiment. Journal of Applied Ecology 47:890–898.

Lobry, C., and J. Harmand. 2006. A new hypothesis to explain the coexistence of *n* species in the presence of a single resource. Comptes Rendus Biologies 329:40–46.

Lobry, C., A. Rapaport, and F. Mazenc. 2006. Sur un modèle densité-dépendant de compétition pour une ressource. Comptes Rendus Biologies 329:63–70.

Logofet, D. O. 1992. Matrices and graphs: stability problems in mathematical ecology. CRC, Boca Raton, FL.

Loreau, M. 2000. Biodiversity and ecosystem functioning: recent theoretical advances. Oikos 91:3–17.

———. 2010. From populations to ecosystems: theoretical foundations for a new ecological synthesis. Princeton University Press, Princeton, NJ.

Loreau, M., S. Naeem, and P. Inchausti. 2002. Biodiversity and ecosystem functioning: synthesis and perspectives. Oxford University Press, Oxford.

MacArthur, R. H. 1970. Species packing and competitive equilibrium for many species. Theoretical Population Biology 1:1–11.

———. 1972. Geographical ecology: patterns in the distribution of species. Princeton University Press, Princeton, NJ.

MacArthur, R. H., and R. Levins. 1967. The limiting similarity, convergence, and divergence of coexisting species. American Naturalist 101:377–385.

Mulder, C. P. H., D. D. Uliassi, and D. F. Doak. 2001. Physical stress and diversity-productivity relationships: the role of positive interactions. Proceedings of the National Academy of Sciences of the USA 98:6704.

O'Connor, M. I., A. Gonzalez, J. E. K. Byrnes, B. J. Cardinale, J. E. Duffy, L. Gamfeldt, J. N. Griffin, et al. 2017. A general biodiversity-function relationship is mediated by trophic level. Oikos 126:18–31.

Parain, E. C., D. Gravel, R. P. Rohr, L.-F. Bersier, and S. M. Gray. 2016. Mismatch in microbial food webs: predators but not prey perform better in their local biotic and abiotic conditions. Ecology and Evolution 6:4885–4897.

Parain, E. C., R. P. Rohr, S. M. Gray, and L.-F. Bersier. 2018. Data from: Increased temperature disrupts the biodiversity–ecosystem

functioning relationship. American Naturalist, Dryad Digital Repository, https://dx.doi.org/10.5061/dryad.hk1h26n.
Perkins, D. M., R. A. Bailey, M. Dossena, L. Gamfeldt, J. Reiss, M. Trimmer, and G. Woodward. 2015. Higher biodiversity is required to sustain multiple ecosystem processes across temperature regimes. Global Change Biology 21:396–406.
Petchey, O. L., P. T. McPhearson, T. M. Casey, and P. J. Morin. 1999. Environmental warming alters food-web structure and ecosystem function. Nature 402:69–72.
Rall, B. C., O. Vucic-Pestic, R. B. Ehnes, M. Emmerson, and U. Brose. 2010. Temperature, predator-prey interaction strength and population stability. Global Change Biology 16:2145–2157.
Rohr, R. P., S. Saavedra, and J. Bascompte. 2014. On the structural stability of mutualistic systems. Science 345:1253497.
Rossberg, A. G. 2013. Food webs and biodiversity: foundations, models, data. Wiley, Chichester.
Rychtecká, T., V. Lanta, I. Weiterová, and J. Lepš. 2014. Sown species richness and realized diversity can influence functioning of plant communities differently. Naturwissenschaften 101:637–644.
Srivastava, D. S., J. Kolasa, J. Bengtsson, A. Gonzalez, S. P. Lawler, T. E. Miller, P. Munguia, T. Romanuk, D. C. Schneider, and M. K. Trzcinski. 2004. Are natural microcosms useful model systems for ecology? Trends in Ecology and Evolution 19:379–384.
Stachová, T., and J. Lepš. 2010. Species pool size and realized species richness affect productivity differently: a modeling study. Acta Oecologica 36:578–586.
Steudel, B., A. Hector, T. Friedl, C. Löfke, M. Lorenz, M. Wesche, and M. Kessler. 2012. Biodiversity effects on ecosystem functioning change along environmental stress gradients. Ecology Letters 15:1397–1405.
Svirezhev, Y. M., and D. O. Logofet. 1983. Stability of biological communities. Mir, Moscow.
Tilman, D., F. Isbell, and J. M. Cowles. 2014. Biodiversity and ecosystem functioning. Annual Review of Ecology, Evolution, and Systematics 45:471–493.
Tilman, D., C. L. Lehman, and K. T. Thomson. 1997. Plant diversity and ecosystem productivity: theoretical considerations. Proceedings of the National Academy of Sciences of the USA 94:1857–1861.
Tilman, D., P. B. Reich, J. Knops, D. Wedin, T. Mielke, and C. Lehman. 2001. Diversity and productivity in a long-term grassland experiment. Science 294:843–845.
Vandermeer, J. H. 1969. The competitive structure of communities: an experimental approach with protozoa. Ecology 50:362–371.
———. 1970. The community matrix and the number of species in a community. American Naturalist 104:73–83.
Vasseur, D. A., J. P. DeLong, B. Gilbert, H. S. Greig, C. D. Harley, K. S. McCann, V. Savage, T. D. Tunney, and M. I. O'Connor. 2014. Increased temperature variation poses a greater risk to species than climate warming. Proceedings of the Royal Society B 281:20132612.
Wilson, W. G., P. Lundberg, D. P. Vázquez, J. B. Shurin, M. D. Smith, W. Langford, K. L. Gross, and G. G. Mittelbach. 2003. Biodiversity and species interactions: extending Lotka-Volterra community theory. Ecology Letters 6:944–952.
Zander, A., L.-F. Bersier, and S. M. Gray. 2017. Effects of temperature variability on community structure in a natural microbial food web. Global Change Biology 23:56–67.
Zander, A., D. Gravel, L.-F. Bersier, and S. M. Gray. 2016. Top predators affect the composition of naive protist communities, but only in their early-successional stage. Oecologia 180:519–528.

References Cited Only in the Online Appendixes

Bastolla, U., M. Lässig, S. C. Manrubia, and A. Valleriani. 2005. Biodiversity in model ecosystems. I. Coexistence conditions for competing species. Journal of Theoretical Biology 235:521–530.
Palamara, G. M., D. Z. Childs, C. F. Clements, O. L. Petchey, M. Plebani, and M. J. Smith. 2014. Inferring the temperature dependence of population parameters: the effects of experimental design and inference algorithm. Ecology and Evolution 4:4736–4750.
R Core Team. 2015. R: a language and environment for statistical computing. R Foundation for Statistical Computing, Vienna.
Saavedra, S., R. P. Rohr, L. J. Gilarranz, and J. Bascompte. 2014. How structurally stable are global socioeconomic systems? Journal of the Royal Society Interface 11:20140693.
terHorst, C. P. 2011. Experimental evolution of protozoan traits in response to interspecific competition. Journal of Evolutionary Biology 24:36–46.

Associate Editor: Sean R. Connolly
Editor: Judith L. Bronstein

The biodiversity–ecosystem functioning experiment was conducted with protozoan species isolated from natural communities inhabiting the water-filled leaves of *Sarracenia purpurea*. The picture is of the Champ Buet field site in Switzerland. Photo credit: L.-F. Bersier.

 DOI: 10.1086/701432

Appendix A from E. C. Parain et al., "Increased Temperature Disrupts the Biodiversity–Ecosystem Functioning Relationship" (Am. Nat., vol. 193, no. 2, p. 227)

Mathematical Derivations

A1. Extension to Multiple Resources

In this section, we explain how the derivation of the Lotka-Volterra model for consumers only (eqq. [3], [4]) can be extended to the case of multiple resources or to a continuous axis of resources. In the case of more than one resource, the Lotka-Volterra model (eq. [1]) extends to

$$\begin{aligned}\frac{dC_i}{dt} &= C_i\left(-m_i - \sum_j \gamma_{ij}C_j + \varepsilon_i \sum_k a_{ik}R_k\right),\\ \frac{dR_k}{dt} &= R_k\left(r_k - \alpha_k R_k - \sum_j a_{jk}C_j\right),\end{aligned} \tag{A1}$$

where the variable C_i denotes the biomass of consumer i and the variable R_k denotes the biomass of the resource k. The parameters of the model are as follows: $m_i > 0$, the mortality rate of consumer i; $a_{ik} > 0$, the attack rate of consumer i on the resource k; $\varepsilon_i > 0$, the efficiency of transforming resource into consumer i (assumed for simplicity to be similar for all resources k); $r_k > 0$, the growth rate of the resource k; $\alpha_k > 0$, the intraspecific competition of the resource k; and γ_{ij}, the nontrophic interactions among consumers i and j (i.e., interference or positive interactions but not the competition for the common resource). As in the case with one resource, we assume the dynamics of the resources to be faster than the dynamics of the consumers, and therefore the consumer-resource dynamic system (A1) can be expressed as a consumer interaction model. The dynamic model among consumers is exactly the same as in the case for one resource (eq. [3]), but the parameters are now given by

$$r_i = -m_i + \varepsilon_i \sum_k a_{ik}\frac{r_k}{\alpha_k} \tag{A2}$$

for the intrinsic growth rate of consumer i in the presence of the resources,

$$\alpha_{ij}^{\text{eff}} = \gamma_{ij} + \varepsilon_i \sum_k \frac{a_{ik}a_{jk}}{\alpha_k} \tag{A3}$$

for the effective interaction between consumers i and j,

$$K_i = \frac{r_i}{\alpha_{ii}^{\text{eff}}} = \frac{-m_i + \varepsilon_i \sum_k a_{ik}\frac{r_k}{\alpha_k}}{\gamma_{ii} + \varepsilon_i \sum_k \frac{a_{ik}a_{ik}}{\alpha_k}} \tag{A4}$$

for the carrying capacity of consumer i in the presence of the resources, and

$$\alpha_{ij} = \frac{\alpha_{ij}^{\text{eff}}}{\alpha_{ii}^{\text{eff}}} = \frac{\gamma_{ij} + \varepsilon_i \sum_k \frac{a_{ik}a_{jk}}{\alpha_k}}{\gamma_{ii} + \varepsilon_i \sum_k \frac{a_{ik}a_{ik}}{\alpha_k}} \tag{A5}$$

for the standardized effective interaction between consumers i and j. These four equations are similar to the ones derived in the case of only one common resource, except that now we must sum all the resources.

In the same manner, we can also extend our framework for a continuous axis of resources. In that case the index k for the resource is replaced by a continuous variable x, and the summations are replaced by integration over the

resource axis (MacArthur and Levins 1967; MacArthur 1970; Logofet 1992; Loreau 2010). The intrinsic growth rate is thus given by

$$r_i = -m_i + \varepsilon_i \frac{r_R}{\alpha_R} \int a_i(x)\, dx, \tag{A6}$$

where $a_i(x)$ is the niche utilization function of consumer i. This function is equivalent to the attack rate, but instead of having a discrete index k, it is a function of the position x on the resource axis. In turn, the effective interaction, the carrying capacity, and the standardized effective interaction are respectively given by

$$\alpha_{ij}^{\text{eff}} = \gamma_{ij} + \frac{\varepsilon_i}{\alpha_R} \int a_i(x) a_j(x)\, dx, \tag{A7}$$

$$K_i = \frac{r_i}{\alpha_{ii}^{\text{eff}}} = \frac{-m_i + \varepsilon_i \frac{r_R}{\alpha_R} \int a_i(x)\, dx}{\gamma_{ij} + \frac{\varepsilon_i}{\alpha_R} \int a_i(x) a_i(x)\, dx}, \tag{A8}$$

and

$$\alpha_{ij} = \frac{\alpha_{ij}^{\text{eff}}}{\alpha_{ii}^{\text{eff}}} = \frac{\gamma_{ij} + \frac{\varepsilon_i}{\alpha_R} \int a_i(x) a_j(x)\, dx}{\gamma_{ii} + \frac{\varepsilon_i}{\alpha_R} \int a_i(x) a_i(x)\, dx}. \tag{A9}$$

With multiple continuous axes of resources (i.e., a multidimensional niche space), the integration in equations (A7) to (A9) becomes a multiple integration over the multidimensional niche space. As explained in Svirezhev and Logofet (1983, p. 193), the integration at the denominator of equation (A9) is the total probability that the consumers i and j meet at one point of the niche axis and thus characterizes the overlap on the niche axis (assuming normalized utilization function). By including the term γ_{ij} for other nontrophic interactions we take into account other encounter events between consumers than only the ones for the common resources. Then, by normalizing the numerator of equation (A9), we obtain the standardized effective interaction α_{ij} of our Lotka-Volterra model (eq. [4]).

Note that in all these extensions, only the precise way of computing the intrinsic growth rate, carrying capacity, and standardized effective interaction changes; the form of the dynamic model (eq. [4]) remains unchanged. Therefore, the form of the BEF model (eq. [11]) is the same, as is the interpretation of ρ, the average standardized interaction. Indeed, the difference between the standardized effective interaction in the one-resource case (eq. [5]), the multiple-resources case (eq. [A5]), and the continuous resource axis case (eq. [A9]) is very minor. We move from the product of the attack rates on the single resource to the sum of this product over all resources, and finally, in the continuous case, the sum is replaced by an integration.

A2. Derivation of the BEF Model from the Consumer-Resource Model

Here, we provide a direct derivation of the BEF model (eq. [11]). We do not assume anymore that the dynamics of the resource are faster than the ones of the consumers and thus that the equilibrium R^* for the consumer can be introduced in the differential equation. We assume only that the system holds a positive equilibrium point for resources and consumers. The starting point is again the consumer-resource Lotka-Volterra model (MacArthur 1970; Logofet 1992; Loreau 2010):

$$\begin{aligned} \frac{dC_i}{dt} &= C_i \left(-m_i - \sum_{j=1}^{S} \gamma_{ij} C_j + \varepsilon_i a_i R \right), \\ \frac{dR}{dt} &= R \left(r_R - \alpha_R R - \sum_{j=1}^{S} a_j C_j \right). \end{aligned} \tag{A10}$$

The parameter, the variables, and the dynamic behavior of the model are described in the main text. For simplicity, we consider here a single resource and S consumers (similar derivations hold for several resources or continuous niche axes). To derive the positive equilibrium values (R^*, C_i^*), we need to solve the system of equations given by setting the terms within the brackets to zero. This leads to the following system of $S + 1$ linear equations:

$$\begin{aligned} m_i &= -\sum_{j=1}^{S} \gamma_{ij} C_j^* + \varepsilon_i a_i R^*, \\ r_R &= \alpha_R R^* + \sum_{j=1}^{S} a_j C_j^*. \end{aligned} \tag{A11}$$

To solve the system, we first extract R^* from the last equation. This results in

$$R^* = \frac{1}{\alpha_R}\left(r_R - \sum_{j=1}^{S} a_j C_j^*\right). \tag{A12}$$

Then, by placing the equation for R^* into the first S equation of the system [A10], we obtain the following set of S linear equations for the consumers' equilibrium:

$$m_i = -\sum_{j=1}^{S} \gamma_{ij} C_j^* + \varepsilon_i a_i \frac{1}{\alpha_R}\left(r_R - \sum_{j=1}^{S} a_j C_j^*\right). \tag{A13}$$

We can rearrange the terms such that

$$-m_i + \varepsilon_i a_i \frac{r_R}{\alpha_R} = \sum_{j=1}^{S}\left(\gamma_{ij} + \frac{\varepsilon_i a_i a_j}{\alpha_R}\right) C_j^*. \tag{A14}$$

This equation is identical to setting to zero the term within the brackets of equation (3). We recognize the intrinsic growth rate of consumer i in $r_i = -m_i + \varepsilon_i a_i r_R/\alpha_R$ and the effective interaction between consumers i and j in $\alpha_{ij}^{\text{eff}} = \gamma_{ij} + \varepsilon_i a_i a_j/\alpha_R$. By making those identifications, we get $r_i = \sum_{j=1}^{S} \alpha_{ij}^{\text{eff}} C_j^*$. Finally, we divide both sides by the effective intraspecific competition term and obtain the following system of S linear equations:

$$K_i = \sum_{j=1}^{S} \alpha_{ij} C_j^*, \tag{A15}$$

with K_i being the carrying capacity of consumer i and α_{ij} being the standardized effective interaction (see the main text). This equation is exactly the same as equation (7), from which we derived the BEF model (eq. [11]).

A3. Interpretation and Modeling of the Average Standardized Interaction ρ

The BEF model for the relative biomass (eq. [11]) is given by

$$\frac{\sum_{i=1}^{S} C_i^*}{\langle K_i \rangle} \approx \frac{S}{1 + (S-1)\rho}. \tag{A16}$$

Figure A1 shows how the relationship between the relative biomass and the number of species is modulated by average standardized interaction ρ. It shows that for $\rho > 1$ the BEF relationship is negative, for $\rho = 1$ the relationship is flat, and for $0 < \rho < 1$ the relationship is positive. Indeed, one can show that the BEF model is a monotonic function converging to the value $1/\rho$. The problem is when one considers a negative value for ρ, that is, when facilitation is predominant in the system. In that case, it is easy to demonstrate that the relative biomass will undergo a vertical asymptote at $S = 1 - 1/\rho$, the point at which the denominator on the left side of equation (A16) equals zero. This is a well-known phenomenon when modeling facilitation with linear functional response in Lotka-Volterra models (Goh 1979; Rohr et al. 2014). If the facilitation is too strong, then the densities will diverge and eventually go to infinity. To cope with this singularity in a linear Lotka-Volterra model, a sensible solution is to dampen the facilitation interaction

with increasing species richness and therefore to impose that ρ increases with the number of species and converges to a positive value. Consequently, we use two models for ρ.

The simplest model considers the average standardized interaction ρ to be independent from the number of species S:

$$\langle \alpha_{ij} \rangle_{i \neq j} = \rho \sim \lambda_1, \tag{A17}$$

where $\lambda_1 > 0$ is a parameter that has to be estimated from the data. The second model considers ρ to depend on S. In this case, an adequate model is given by

$$\langle \alpha_{ij} \rangle_{i \neq j} = \rho \sim \lambda_1 - \frac{\lambda_2}{S}, \tag{A18}$$

where $\lambda_1 > 0$ and $\lambda_2 > 0$ are parameters that have to be estimated from the data. The extra term λ_2/S represents facilitation, which must decrease with species richness to avoid singularity in the Lotka-Volterra model.

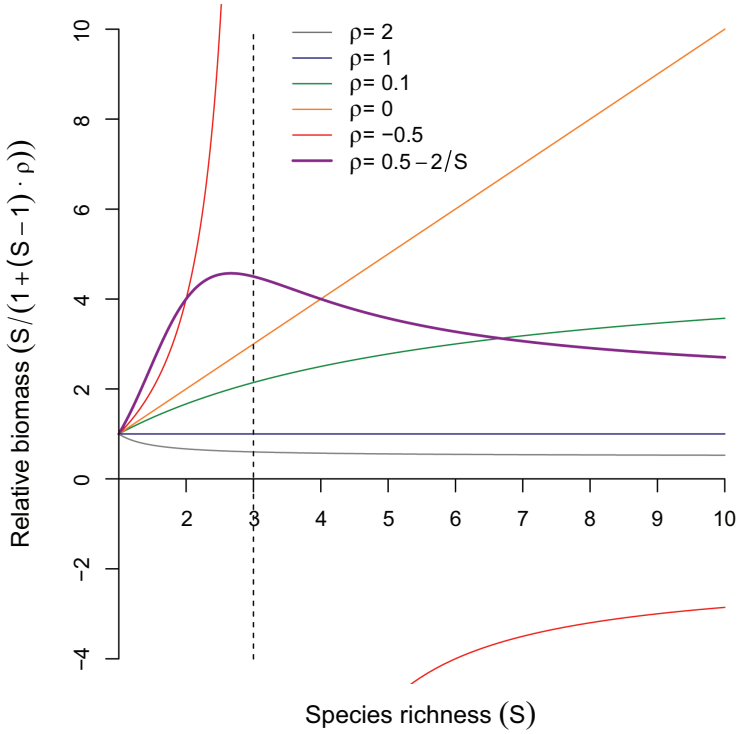

Figure A1: Behavior of the biodiversity–ecosystem functioning model (eq. [11]) for different values of the average standardized interaction ρ (plain lines). Note that for $\rho < 0$ (i.e., the system is dominated by facilitation), the model exhibits a singularity (vertical dashed line). A solution is to have ρ depend on species richness S (thick violet line).

A4. The BEF Relationship with Species Extinctions

In the case where extinctions occur, it is challenging to provide a theoretical model for the BEF relationship. First, we cannot use equation (7), which describes the positive equilibrium point, since only a subset of X species from our original set of S species will have a positive biomass at equilibrium. Therefore, we have to rewrite equation (7) for that subset only, that is,

$$\begin{aligned} K_1 &= 1 \cdot C_1^* + \cdots + \alpha_{1X} C_X^* \\ &\vdots \qquad\quad \vdots \qquad\quad \vdots \\ K_X &= \alpha_{X1} C_1^* + \cdots + 1 \cdot C_X^* \end{aligned} \tag{A19}$$

Here we assume, with a renumbering of the species, that $C_1^* > 0, \ldots, C_X^* > 0, C_{X+1}^* = 0, \ldots, C_S^* = 0$. Then, with extinction, we can derive a BEF relationship of the same form as equation (11):

$$\frac{\sum_{i=1}^{X} C_i^*}{\langle K_i \rangle} \approx \frac{S}{1 + (S-1)\rho_X}, \tag{A20}$$

where $\langle K_i \rangle$ is the average carrying capacity of the X surviving species and ρ_X denotes the average standardized interaction of the subset of those X surviving species.

If the selection of the surviving species is random, the approximation $\rho_x \approx \rho$ can be used and the model could apply for the new subset of species. The difficulty of including extinctions in the model occurs when species are selected by a dynamic process, which is likely the case. Here, the average niche overlap ρ_X of the X surviving species cannot be approximated by the average standardized interaction ρ of the S species, that is, $\rho_x \not\approx \rho$. If species are selected, it may be expected that the average standardized interaction for the surviving species is lower than the one for all species. The rationale behind this is that a set of species with a lower level of competition is more likely to coexist than a set of species with a larger level of competition (Vandermeer 1970; Bastolla et al. 2005; Saavedra et al. 2014). This subset of species will have a lower average standardized interaction than what would be expected by chance, which is challenging to model as it will depend on the particular species composition.

Appendix B from E. C. Parain et al., "Increased Temperature Disrupts the Biodiversity–Ecosystem Functioning Relationship" (Am. Nat., vol. 193, no. 2, p. 227)

Effect of Temperature Variability

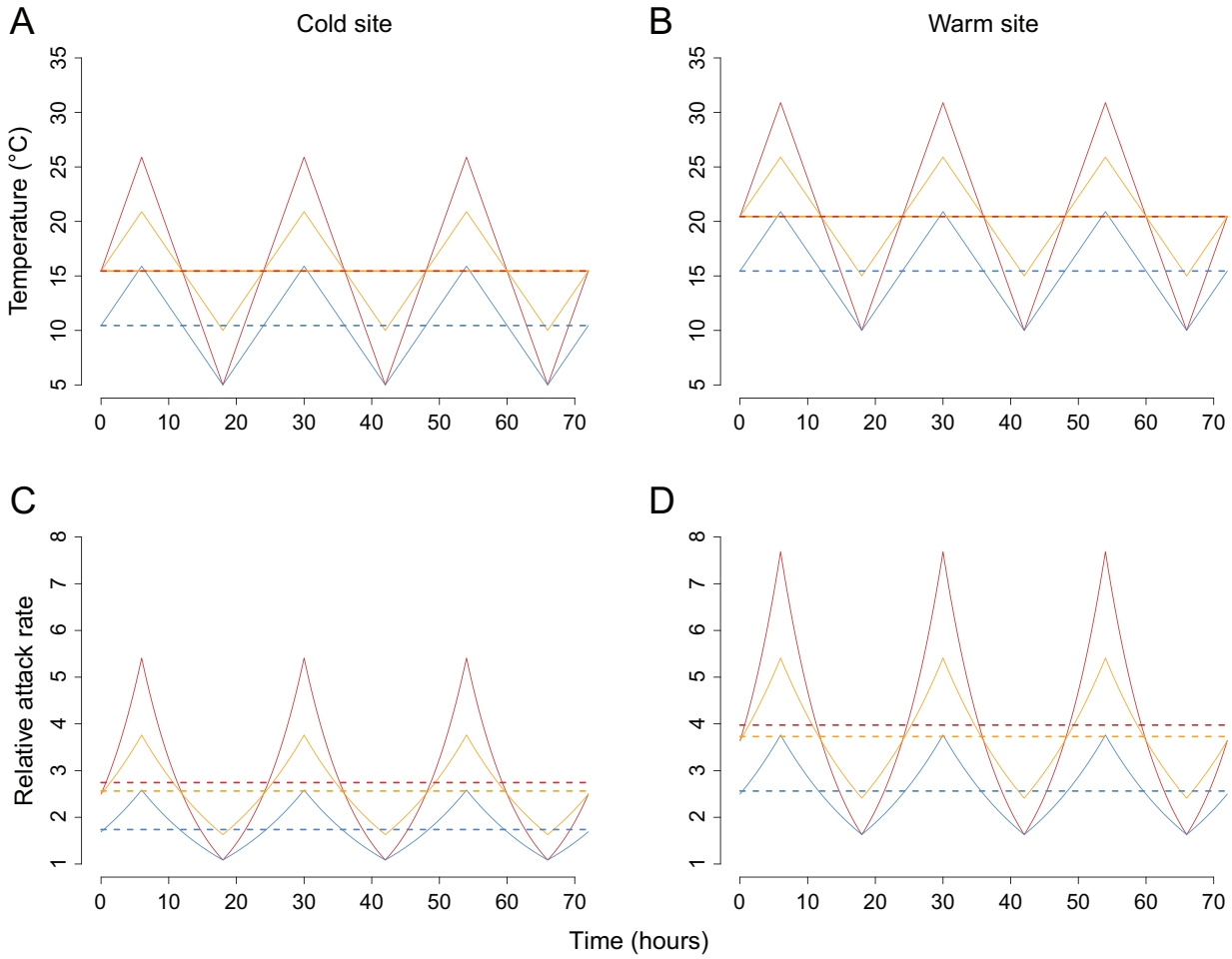

Figure B1: Expected effects of increased temperature on the relative attack rate for the two sites. *A* and *B* show the different temperature treatments that we used in our experiment. The solid blue lines represent the local conditions (*lc*), the solid orange lines represent the high-temperature treatment (*t5*), and the solid red lines represent the high average temperature and variation treatment (*hv*). The dashed lines represent the average temperature for each temperature treatment with similar colors as described before. *D* and *C* show the relative attack rate responses for the three temperature treatments at the two sites. Lines and colors represent the same as described above. This figure shows that the average attack rate increases with temperature increase. However, the *hv* treatment increases the attack rate to an even greater extent. A site difference is also shown in this figure, with the attack rate higher at the warm site than at the cold site. This result can be explained by Jensen's inequality for the nonlinear relationship between attack rate and temperature (see fig. 1*A*).

 DOI: 10.1086/701432

Appendix C from E. C. Parain et al., "Increased Temperature Disrupts the Biodiversity–Ecosystem Functioning Relationship" (Am. Nat., vol. 193, no. 2, p. 227)

Experimental Setting

Field Sites and Sampling

The protozoan species used in our experiment were collected from *Sarracenia purpurea* leaves located at a warm site and a cold site in Switzerland (warm site: Champ Buet [CB], 46°36′50″N, 6°34′50″E, minimum June temperature of 10°C, maximum June temperature of 20.9°C, 500 m asl; cold site: Les Tenasses [LT], 46°29′29″N, 6°55′16″E, minimum June temperature of 7.5°C, maximum June temperature of 18.4°C, 1,200 m asl). Note that in Europe, these communities are mainly composed of protozoans and bacteria that form two trophic levels (consumers and resources, respectively). At the beginning of the growing season, we marked approximately 50 leaves at both field sites that were at the same growing stage and close to opening. Two weeks later, we sampled the water inside the 50 leaves using a 1-mL pipette and sterile tips. These 15 days were necessary to allow for a sufficient amount of time for the leaves to fill with water and for the community to establish. The water from all leaves was pooled in a 1-L autoclaved Nalgene bottle (one bottle per site). The Nalgene bottles containing the *S. purpurea* water from the two sites were brought back to the laboratory and chilled at 4°C overnight to slow community dynamics.

Isolating Protozoans

After observing the protozoan community composition of the two sites under the microscope (inverted Olympus microscope; zoom, ×100), we selected six protozoan morphospecies per site. The morphospecies that were selected were common and in high densities in the communities and were functionally similar between the two sites. Among the six morphospecies, we selected three ciliates and three flagellates.

The isolation of each protozoan morphospecies occurred by sampling 100 μL of the communities and creating aliquots of the sample until a subsample of water was found in which the density of the target protozoan morphospecies was the highest. We then serially diluted this sample with sterile deionized water until we obtained a sample that contained five or fewer individuals from the target morphospecies and no other protozoan species. This procedure ensured that each within-site morphospecies was equivalent to only one species and limited the likelihood of contamination by other protozoan species. This sample was then transferred into a microcentrifuge tube filled with a mixture of 1 mL of sterilized deionized water and 100 μL of fish food (made of a Tetramin fish food solution; Tetra Holding, Blacksburg, VA), according to the protocol given in terHorst (2011). All of the isolated populations for the 12 species (six species per site) were grown in incubators mimicking the temperature of their site of origin and followed during 1 week to determine whether they had reached a high density (at least 500 ciliate individuals and 5,000 flagellate individuals per milliliter) and that no contamination had occurred. In the case of contamination, the isolation process was repeated.

Experimental Design

We first grew the 12 morphospecies independently using three experimental temperature treatments (see below) to obtain information about their growth rate and carrying capacity. The experimental design of this first part of the experiment was as follows: two origins (CB and LT), three temperature treatments, and six morphospecies (three ciliates, three flagellates), with a total of 36 treatments replicated five times, resulting in 180 samples. The densities of the different morphospecies were measured on days 2, 4, and 6.

We then used the information about the growth rate of each morphospecies to build our communities for the experiment. These communities were composed of three levels of complexity (two, four, or six morphospecies) and were always composed of an equal number of ciliate and flagellate morphospecies. For practical reasons, it was not possible to include all possible combinations of morphospecies in the experiment. We used the maximal growth rate

(r_{max}) of each morphospecies in order to choose among the possible combinations (see table C1). Each of the different combinations of community complexity were then grown using the three different temperature treatments, so that the experimental design consisted of two origins × three temperature treatments × nine levels of complexity × four replicates, for a total of 216 samples.

The temperature treatments (see fig. B1*A* and B1*B*) that we applied throughout the course of the experiment were as follows: (1) local conditions (*lc*)—the average June temperature of the two sites according to 30 years of data acquired by WorldClim (http://www.worldclim.org; CB average temperature, 15.5°C; LT average temperature, 10.3°C; daily amplitude of 10°C); (2) high temperature (*t5*)—an increase of 5°C in the average June temperature for both sites but no change in temperature variation (amplitude of 10°C); and (3) higher average temperature and variation (*hv*)—an increase of 5°C in the average June temperature and an increase in the variation (amplitude of 20°C; for CB, average temperature of 20.5°C, minimum temperature of 10°C, maximum temperature of 30.9°C; for LT, average temperature of 15.5°C, minimum temperature of 5°C, maximum temperature of 25.9°C). Each community was placed at the same time in the incubators that corresponded to its origin (three incubators for each origin). Note that the change in daily temperature in the experiment is in the natural range experienced by the communities (the maximum daily amplitude measured at the field sites with a data logger inside the leaves was approximately 25°C, a regime that occurred during 1 week).

Experimental Setup

At the beginning of the experiments, 50-mL macrocentrifuge tubes were filled with 10 mL of sterilized deionized water and 1 mL of a solution of autoclaved Tetramin fish food (terHorst 2011; concentration of 1 mg of solid fish food in 1 mL of deionized water). The initial densities of the protozoans were adjusted according to their body size to obtain approximately similar biomass: we added 500 flagellates and 50 ciliates per tube (except for one ciliate morphospecies from CB where the initial density was 10 individuals due to their bigger size compared with the other ciliate protozoans). Fish food was added at the beginning of the experiment as the basal resource for the bacteria that arrived in the system with the protozoans. By adding this quantity of basal resources, bacteria were able to increase and maintain their densities throughout the experiment.

Monitoring

The density of each protozoan species was measured by sampling an aliquot of 100 μL (1% of the total volume; see Palamara et al. 2014) of the communities and counting the protozoans under an inverted microscope using a Thoma cell microscope plate. When the density was too low to use the Thoma cell accurately, the individuals were counted through the entire 22 × 22-mm coverslip. The biomass of each protozoan morphospecies was measured on days 2, 4, and 6 after the beginning of the experiments; only data from day 6 were used in the biodiversity–ecosystem functioning (BEF) relationship. Body density was assumed to be the same for all morphospecies, so biomass was measured as biovolume. Biovolume was measured at the start of the experiment in the local conditions. We did not measure biovolume during the experiment. Note that we did not observe any obvious change in body size, as has been observed in the presence of competitors (terHorst 2011). Although we cannot exclude the possibility that a change in biovolume of some morphospecies in the course of the experiment may have altered some of the BEF relationships, it is very unlikely that this potential effect could invalidate our main conclusion, that is, a weakening of the BEF relationship with temperature. First, the results of terHorst (2011) indicate that morphospecies selected in polyculture did not change in body size when in the presence of competitors (their fig. 3*b*); our morphospecies were selected from polycultures. Second, if temperature affects body size, it should do it very differently for the different morphospecies to affect the BEF relationships. If the effect of temperature is the same for all species (i.e., a similar proportional change in body size), it will not change the slope of the BEF relationships, only the intercepts for total biomass.

Table C1: Chosen combinations of species for the different diversity levels

	Ciliates	Flagellates
Two species	Highest r_{max}	Highest r_{max}
	Lowest r_{max}	Lowest r_{max}
	Average r_{max}	Average r_{max}
	Highest r_{max}	Lowest r_{max}
Four species	Highest r_{max} + lowest r_{max}	Highest r_{max} + lowest r_{max}
	Highest r_{max} + average r_{max}	Highest r_{max} + average r_{max}
	Average r_{max} + lowest r_{max}	Average r_{max} + lowest r_{max}
	Average r_{max} + lowest r_{max}	Highest r_{max} + average r_{max}
Six species	The three ciliates	The three flagellates

Note: Each of the nine combinations was assembled for the two origins and the three temperature treatments and was replicated four times (for a total of 216 multispecies observations).

 DOI: 10.1086/701432

Appendix D from E. C. Parain et al., "Increased Temperature Disrupts the Biodiversity–Ecosystem Functioning Relationship" (Am. Nat., vol. 193, no. 2, p. 227)

Fitted Biodiversity–Ecosystem Functioning (BEF) Relationship to Empirical Data

We used nonlinear least square regression to fit the BEF model (eq. [11]; right formulation) to empirical data, with equation (A17) or (A18) used for the average standardized interaction. All models were fitted with the function nls of R (R Core Team 2015). For model selection, we provide the Akaike information criterion (AIC) and the Bayesian information criterion (BIC). Because AIC is known to favor overfitting, we based model choice on the BIC to select between models (A17) and (A18).

The right formulation of model (11) is for relative biomass (i.e., biomass in polyculture divided by average biomass in monocultures; see fig. 2 and tables 1 and 2). We also fitted the model to the total biomass (i.e., biomass in polyculture), which is the common currency for BEF analyses (fig. 4). In this case, the statistical model corresponds to the left formulation in equation (11). In this setting, the average carrying capacity was considered a free parameter estimated from the data (λ_0 in table D2).

Table D1: Comparisons of the Akaike information criterion (AIC) and the Bayesian information criterion (BIC) for the two models of average standardized interaction (eqq. [A17], [A18]) for the relationship between total biomass and species richness (fig. 4)

Site, temperature treatment	Model: $\rho \sim \lambda_1$		Model: $\rho \sim \lambda_1 - \lambda_2/S$	
	AIC	BIC	AIC	BIC
Cold:				
lc	1,119	1,125	1,109	**1,117**
t5	1,424	**1,431**	1,425	1,434
hv	1,427	**1,434**	1,430	1,438
Warm:				
lc	1,421	**1,427**	1,423	1,432
t5	1,325	**1,331**	1,327	1,335
hv	991	**997**	993	1,001

Note: We based model choice on the BIC, with values of the best model in boldface type. *hv* = higher average temperature and variation; *lc* = local conditions; *t5* = high temperature.

Table D2: Estimated parameters of the best model in table D1 for the relationship between total biomass and species richness (see fig. 4)

Site, temperature treatment, parameter	Estimate	SE	*P*
Cold:			
lc:			
λ_0	1,287	466	...
λ_1	.130	.053	<.001
λ_2	1.513	.280	<.001
t5:			
λ_0	14,749	2,661	...
λ_1	.455	.188	.004
hv:			
λ_0	14,591	3,986	...
λ_1	.426	.148	<.001
Warm:			
lc:			
λ_0	13,907	1,569	...
λ_1	.172	.062	<.001
t5:			
λ_0	14,682	1,805	...
λ_1	.837	.221	.461
hv:			
λ_0	12,622	2,022	...
λ_1	1.950	1.037	.360

Note: Compared with the models of table 1, the response variable is total biomass (not relative biomass). We considered the average carrying capacity of the biodiversity–ecosystem functioning model (eq. [11]) as a parameter to be estimated: $\langle K_i \rangle \sim \lambda_0$. The *P* values are computed as in table 1. We do not provide *P* values for λ_0 as we are not interested in testing them. *hv* = higher average temperature and variation; *lc* = local conditions; *t5* = high temperature.

 DOI: 10.1086/701432

Appendix E from E. C. Parain et al., "Increased Temperature Disrupts the Biodiversity–Ecosystem Functioning Relationship" (Am. Nat., vol. 193, no. 2, p. 227)

Species Extinctions in the Experiment

We analyzed the number of extinctions with a binomial generalized linear model (logistic regression) for both sites separately. The analysis was performed with the function glm of R (R Core Team 2015). We used species richness and temperature treatment as explanatory variables. The latter variable was coded as an ordered factor, with $lc < t5 < hv$; we considered only the linear term for this variable. Note that there was no evidence of interaction between both factors at both sites. Because of the low frequencies for the number of extinctions, all reported P values must be interpreted with caution. At the warm site, we observed zero extinctions for the normal temperature treatment in all levels of species richness. This explains the large standard errors of the intercept and of the variable *temp*. Using Markov chain Monte Carlo–based approximate exact conditional inference for logistic regression models did not solve this problem. The main results are that extinction frequency increases with species richness; however, these results were inconclusive with temperature treatment (more extinctions occurred at the warm site with increased treatment intensity, but extinctions tended to become less frequent at the cold site).

Table E1: Frequency of experimental tubes without (no) and with (yes) species extinctions

Site, temperature treatment, extinctions	No. species			
	1	2	4	6
Cold site (Les Tenasses):				
lc:				
No	28	13	11	1
Yes	2	3	5	3
t5:				
No	30	16	16	2
Yes	0	0	0	2
hv:				
No	30	16	15	4
Yes	0	0	1	0
Warm site (Champ Buet):				
lc:				
No	30	16	16	4
Yes	0	0	0	0
t5:				
No	30	16	13	3
Yes	0	0	3	1
hv:				
No	30	13	3	0
Yes	0	3	13	4

Note: We observed 40 cases of extinction in the 396 tubes. In six cases, two species became extinct (four times with four species and twice with six species). All other cases involved one species. *hv* = higher average temperature and variation; *lc* = local conditions; *t5* = high temperature.

Table E2: Results of binomial generalized linear model analyses for the occurrence of extinctions as a function of species richness *S* and temperature treatment *temp* for the cold site and the warm site

Site, parameter	Estimate	SE	*z*	*P*
Cold site (Les Tenasses):				
Intercept	−5.42	.887	−6.11	<.001
S	.77	.196	3.93	<.001
temp	−2.27	.790	−2.87	.004
Warm site (Champ Buet):				
Intercept	−13.02	572.5	−.023	.98
S	1.47	.276	5.27	<.001
temp	15.29	1,214.6	.013	.99

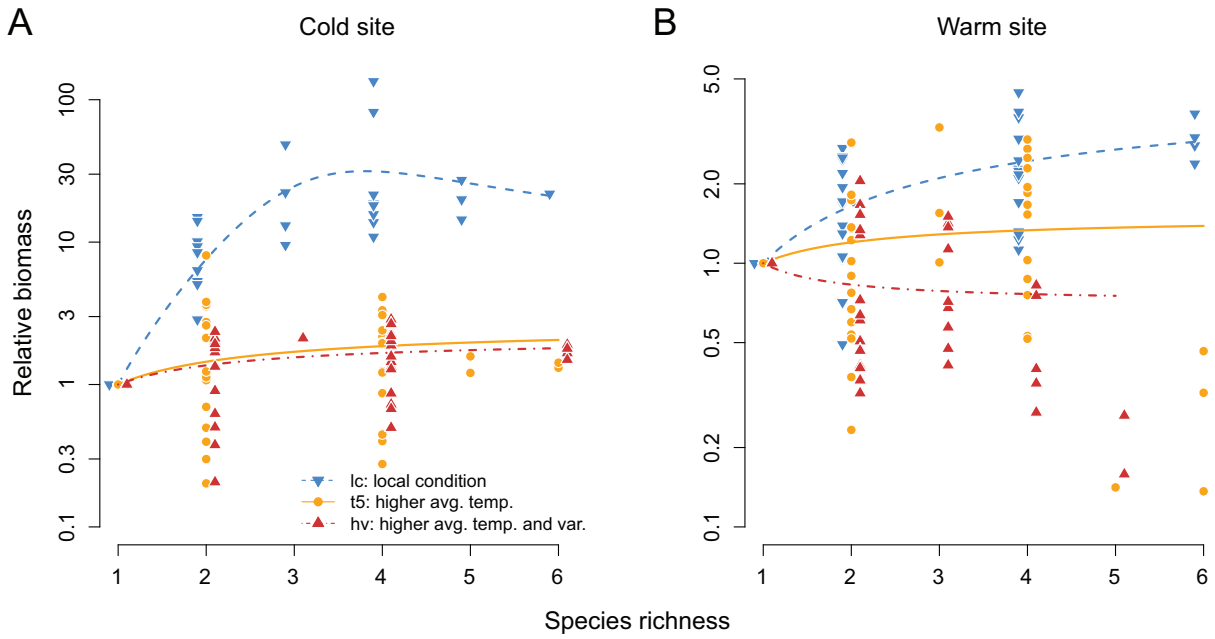

Figure E1: Same as figure 2, but including the cases with extinctions.

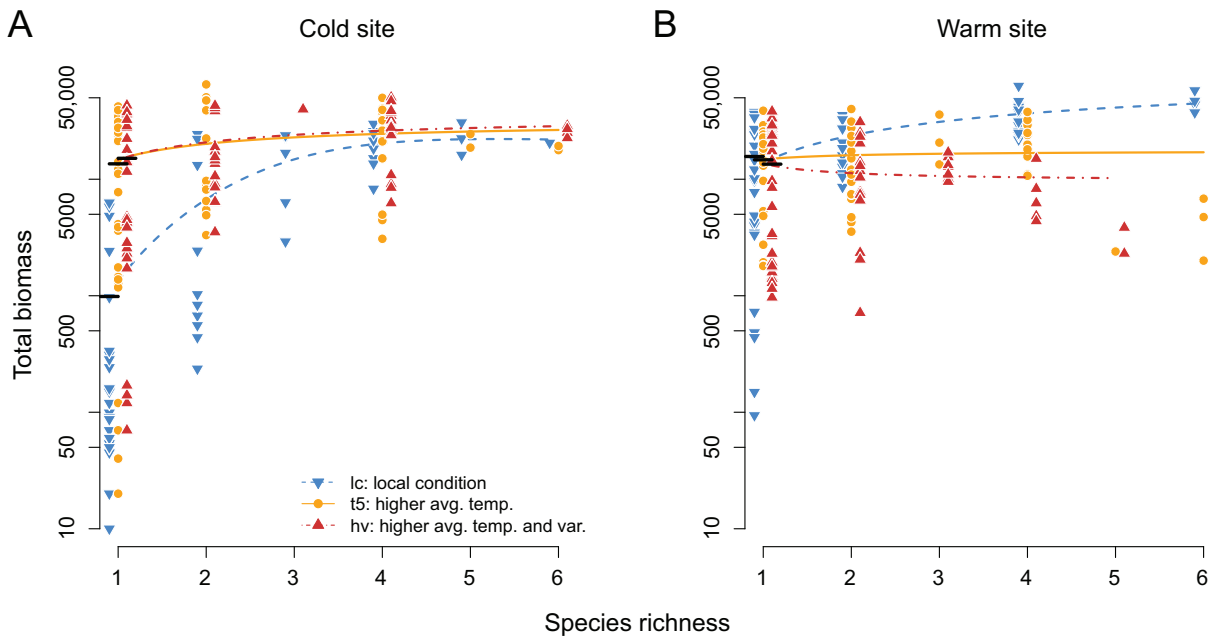

Figure E2: Same as figure 4, but including the cases with extinctions.

Table E3: Same as table 2 (relative biomass), but including the cases with extinctions

Site, temperature treatment	Model: $\rho \sim \lambda_1$		Model: $\rho \sim \lambda_1 - \lambda_2/S$	
	AIC	BIC	AIC	BIC
Cold:				
lc	317.5	320.5	305.4	**309.9**
t5	140.9	**144.1**	138.1	142.8
hv	78.0	**81.1**	79.9	84.6
Warm:				
lc	91.1	**94.3**	93.1	97.9
t5	97.6	**100.7**	93.9	103.7
hv	51.0	**54.0**	50.8	55.3

Note: The Bayesian information criterion (BIC) values for the best model are in boldface type. AIC = Akaike information criterion; *hv* = higher average temperature and variation; *lc* = local conditions; *t5* = high temperature.

Table E4: Same as table 3 (relative biomass), but including the cases with extinctions

Site, temperature treatment, parameter	Estimate	SE	*P*
Cold:			
lc: λ_1	.154	.062	<.001
lc: λ_2	1.781	.242	<.001
t5: λ_1	.384	.126	<.001
hv: λ_1	.467	.065	<.001
Warm:			
lc: λ_1	.213	.036	<.001
t5: λ_1	.666	.134	.013
hv: λ_1	1.411	.226	.069

Note: *hv* = higher average temperature and variation; *lc* = local conditions; *t5* = high temperature.

Table E5: Same as table D1 (total biomass), but including the cases with extinctions

Site, temperature treatment	Model: $\rho \sim \lambda_1$		Model: $\rho \sim \lambda_1 - \lambda_2/S$	
	AIC	BIC	AIC	BIC
Cold:				
lc	1,345	1,352	1,335	**1,343**
t5	1,467	**1,474**	1,468	1,478
hv	1,449	**1,456**	1,451	1,461
Warm:				
lc	1,420	**1,427**	1,423	1,432
t5	1,412	**1,418**	1,414	1,422
hv	1,412	**1,418**	1,413	1,422

Note: We based model choice on the Bayesian information criterion (BIC), with values of the best model in boldface type. AIC = Akaike information criterion; *hv* = higher average temperature and variation; *lc* = local conditions; *t5* = high temperature.

Table E6: Same as table D2 (total biomass), but including the cases with extinctions

Site, temperature treatment, parameter	Estimate	SE	*P*
Cold:			
lc:			
λ_0	1,334	485	
λ_1	.111	.034	<.001
λ_2	1.428	.217	<.001
t5:			
λ_0	14,807	2,625	
λ_1	.471	.184	.004
hv:			
λ_0	14,684	2,256	
λ_1	.417	.145	<.001
Warm			
lc:			
λ_0	13,907	1,569	
λ_1	.172	.062	<.001
t5:			
λ_0	14,801	1,830	
λ_1	.843	.216	.466
hv:			
λ_0	11,558	1,948	
λ_1	1.415	.439	.345

Note: *hv* = higher average temperature and variation; *lc* = local conditions; *t5* = high temperature.